NRC Research Press

ARTICLE

Investigation of the influence of natural fractures and in situ stress on hydraulic fracture propagation using a distinct-element approach

N. Zangeneh, E. Eberhardt, and R.M. Bustin

Abstract: Hydraulic fracturing is the primary means for enhancing rock mass permeability and improving well productivity in tight reservoir rocks. Significant advances have been made in hydraulic fracturing theory and the development of design simulators; however, these generally rely on continuum treatments of the rock mass. In situ, the geological conditions are much more complex, complicated by the presence of natural fractures and planes of weakness such as bedding planes, joints, and faults. Further complexity arises from the influence of the in situ stress field, which has its own heterogeneity. Together, these factors may either enhance or diminish the effectiveness of the hydraulic fracturing treatment and subsequent hydrocarbon production. Results are presented here from a series of two-dimensional (2-D) numerical experiments investigating the influence of natural fractures on the modeling of hydraulic fracture propagation. Distinct-element techniques applying a transient, coupled hydromechanical solution are evaluated with respect to their ability to account for both tensile rupture of intact rock in response to fluid injection and shear and dilation along existing joints. A Voronoi tessellation scheme is used to add the necessary degrees of freedom to model the propagation path of a hydraulically driven fracture. The analysis is carried out for several geometrical variants related to hypothetical geological scenarios simulating a naturally fractured shale gas reservoir. The results show that key interactions develop with the natural fractures that influence the size, orientation, and path of the hydraulic fracture as well as the stimulated volume. These interactions may also decrease the size and effectiveness of the stimulation by diverting the injected fluid and proppant and by limiting the extent of the hydraulic fracture.

Key words: hydraulic fracturing, natural fracture, in situ stress, distinct-element method, Voronoi, invaded and dilated zone, angle of approach, fracture arrest, fracture offset.

Résumé : La fracturation hydraulique et le principal moyen d'améliorer la perméabilité des massifs rocheux et la productivité des puits dans les roches-réservoirs étanches. Des avancées importantes ont été réalisées sur le plan théorique dans le domaine de la fracturation hydraulique et dans l'élaboration de simulateurs de conception. Cependant, ceux-ci reposent habituellement sur des traitements en continu du massif rocheux. Les conditions géologiques in situ sont beaucoup plus complexes en raison de la présence de fractures naturelles et de plans de faiblesse tels que des plans de litage, des failles et des diaclases. Cette complexité est accrue du fait de l'influence du champ de contrainte in situ et de sa propre hétérogénéité. Ensemble, ces facteurs ont le pouvoir d'augmenter ou de diminuer l'efficacité du traitement de fracturation hydraulique et de la production hydrocarbure qui s'ensuit. Les résultats sont ici décrits à partir d'une série d'expériences numériques bidimensionnelles visant à étudier l'influence des fractures naturelles sur la modélisation de la propagation des fractures obtenues voie hydraulique. Des méthodes d'éléments distincts consistant à appliquer une solution transitoire à la fois hydraulique et mécanique sont évaluées par rapport à leur capacité à prendre en compte de la rupture en traction de la roche intacte en réponse à l'injection de fluide et du cisaillement et de la dilatation le long de diaclases existantes. Un diagramme de Voronoï est utilisé afin d'obtenir les degrés de liberté nécessaires à la modélisation de la voie de propagation d'une fracture hydraulique. L'analyse est effectuée pour plusieurs variantes géométriques liées à des scénarios géologiques hypothétiques simulant un réservoir de gaz de schiste fracturé de manière naturelle. Les résultats montrent que des interactions majeures se produisent avec les fractures naturelles, qui influencent la taille, l'orientation et la voie de propagation de la fracture hydraulique ainsi que le volume stimulé. Ces interactions ont également pour effet de diminuer la taille et l'efficacité de la stimulation en déviant le fluide et l'agent de soutènement injectés et en limitant l'agrandissement de la fracture hydraulique. [Traduit par la Rédaction]

Mots-clés : fracturation hydraulique, fracture naturelle, contrainte in situ, méthode des éléments distincts, Voronoi, zone envahie et dilatée, angle d'approche, arrêt ou déviation de la fracture.

Received 2 October 2013. Accepted 8 October 2014.

N. Zangeneh,* E. Eberhardt, and R.M. Bustin. Earth, Ocean & Atmospheric Sciences, The University of British Columbia, Vancouver, BC, Canada.
Corresponding author: Neda Zangeneh (e-mails: neda@eos.ubc.ca, NZangeneh@slb.com).
*Present address: Schlumberger, Petro Technical Services, 1325 South Dairy Ashford, Houston, TX 77077, USA.

Fig. 1. Examples of natural fractures present in shales: (*a*) Devonian shale outcrop from northeastern British Columbia, (*b*) borehole image log from a horizontal well through the Muskwa – Otter Park formation, (*c*) open and partially open fractures in retrieved core, and (*d*) closed fractures in core samples from the Muskwa – Otter Park formation (after Reine and Dunphy 2011).

Hydraulic fracture modeling and shale gas reservoirs

Guided by more than 60 years of experience in its use, hydraulic fracturing represents a proven means to enhance rock mass permeability in tight reservoir rocks, assisting in more efficient hydrocarbon production and increased ultimate economic recovery. Their design involves (*i*) characterizing the geology and rock mass properties, (*ii*) estimating the orientation and magnitudes of the principal stresses, and (*iii*) selecting the properties of the injection fluids and proppant (Economides and Nolte 2000). Significant advances have been made in hydraulic fracturing theory and the development of design simulators over the past decades; however, these advances have largely focussed on continuum treatments of the rock mass, concentrating on crack tip processes. In the two introductory models upon which early hydraulic fractures were designed, the PKN (Perkins and Kern 1961; Nordgren 1972) and KGD (Khristianovitch and Zheltov 1955; Geertsma and de Klerk 1969), the rock mass is assumed to be a homogeneous, isotropic, linear elastic continuum. Many subsequent models and industry design software (e.g., Fracpro, GOHFER, MFRAC) have adopted these assumptions (e.g., Cleary 1980; Barree 1983; Shaffer et al. 1984; Ventura 1985; Meyer 1989; Mohaghegh et al. 1999; Dong and de Pater 2002; Reynolds et al. 2004).

In actuality, however, the geology of the reservoir rocks, especially those related to unconventional resources (e.g., shale gas) involve heterogeneous, anisotropic rock masses containing numerous natural fractures and other defects that serve as planes of weakness. Geological discontinuities such as joints, bedding planes, and shear fractures and faults are commonly found in shale gas reservoirs (e.g., Fig. 1). Field experience in shale gas reservoirs suggests a significant interaction between natural fractures and induced hydraulic fractures. In a review of data derived from a large number of hydraulic fracture treatments, Cleary et al. (1991) cite the presence of natural fractures as the key reason for misinterpreted data and arrested fracture propagation. Numerous other studies also show that parameter uncertainty due to the presence of natural fractures can significantly impact hydraulic fracture designs (e.g., Palisch et al. 2007, Moos and Barton 2008, Zhang et al. 2009, Dusseault et al. 2011, Meyer et al. 2013). Microseismic monitoring provides further field-based evidence that existing natural fractures favorably oriented for shear will activate in response to interactions with a hydraulic fracture treatment (e.g., Rutledge et al. 2004; Wessels et al. 2011, Williams-Stroud et al. 2012). Thus, the influence of natural fractures on the final performance of a hydraulic fracture treatment is significant and needs to be considered in its design.

To meet the objective of modeling the effect of natural fractures on hydraulic fracturing performance, the model should include a representative number of oriented discontinuities to more accurately represent the planes of weakness that exist within the reservoir rock mass. These discontinuities include weak bedding planes and persistent joints forming along bedding that typically represent the dominant discontinuity set. Other nonpersistent natural fracture sets include cross joints that are subnormal to bedding and fractures at acute angles that are fold-related as a result of tectonic forces (Nelson 2001). Together, these discontinuity sets form a network of pre-existing fractures of varying persistence, spacing, dip angle, and direction relative to the orientation of the present-day in situ stress field and injection wellbore.

Consequently, researchers have begun to investigate using discontinuum methods such as discrete- and distinct-element methods. Early work by Hazzard et al. (2002) and later Gil et al. (2010) has examined using Itasca's Particle Flow Code (PFC) to model hydraulic fracturing, showing that the model is capable of capturing the true physics of injection into low-permeability formations. Damjanac et al. (2010) used the PFC to model hydraulic fracturing in a naturally fractured reservoir, embedding a discrete fracture network representing natural fractures into a bonded-particle model to simulate both tensile failure of intact rock and shearing of pre-existing fractures. Studies comparing model simulations of hydraulic fracturing with laboratory experiment and field observations of microseismic locations, magnitudes, and source mechanisms have helped validate the PFC discrete-element approach (Zhao and Young 2011; Yoon et al. 2013; Zang et al. 2013).

Researchers have also investigated bonded-block models using Itasca's Universal Distinct Element Code (UDEC) and 3DEC code. McLennan et al. (2010) used 3DEC to model and assess complex fracture growth, and the associated production, across a network of vertically dipping orthogonal fractures. Choi (2012) used UDEC to compare several methods for determining the shut-in pressure during hydraulic fracturing, because the shut-in pressure is not considered certain, owing to the relationship between the behaviour of hydraulic fractures and the remote in situ stress. Hamidi and Mortazavi (2012) used 3DEC for small models to study the effects of different fracture fluid properties and fluid rates, in situ stress states, and rock mass properties on hydraulic fracture propagation. Zangeneh et al. (2012) further demonstrated the potential value of UDEC for simulating hydraulic fracturing, comparing different injection schedules from adjacent wellbores (e.g., zipperfrac, simulfrac), and showed that stress and pore pressure perturbations from multiple hydraulic fractures may impact wellbore spacing and injection optimization. Zangeneh et al. (2013) applied this approach to model fault slip and was able to use UDEC to estimate the energy release associated with induced seismicity.

Numerical modeling methodology

The two-dimensional (2-D) commercial distinct-element code UDEC (Itasca Consulting Group 2011) is used here to simulate the response of a jointed rock mass subject to static loading and hydraulic injection. The distinct-element method is a Lagrangian numerical technique in which the problem domain is divided through by discontinuities of variable orientation, spacing and persistence, which may undergo large deformations in shear and opening in response to a change to the modeled stresses. UDEC can simulate the progressive failure associated with crack initiation and propagation by the breaking of pre-existing contacts between the pre-defined joint bounded blocks. The blocks are deformable, but they remain intact. A detailed discussion of the distinct-element method is presented by Cundall and Hart (1992).

A limiting factor in modeling stress-induced fracturing using UDEC is that all potential fracture pathways must be pre-defined. To counter this limitation and provide added degrees of freedom for fracture propagation, a Voronoi tessellation scheme can be used to generate randomly sized polygonal blocks (Fig. 2). These Voronoi contacts can then be assigned strengths equivalent to weak intact rock and are referred to here as "incipient fractures". These are used in this study to provide a background network of potential fracture pathways to model the propagation path of a hydraulically driven fracture. Superimposed on this background can be discontinuities of a set dip angle, spacing, and persistence with assigned zero cohesion and tensile strength values, representing natural pre-existing fractures in the rock mass. This integrated system was developed and tested here to enable modeling

Fig. 2. (*a*) Distinct-element discretization in UDEC, using Voronoi tessellation to represent a network of natural fractures intersecting with a background network of incipient fractures and (*b*) coupled hydromechanical logic used for modeled natural and incipient fractures.

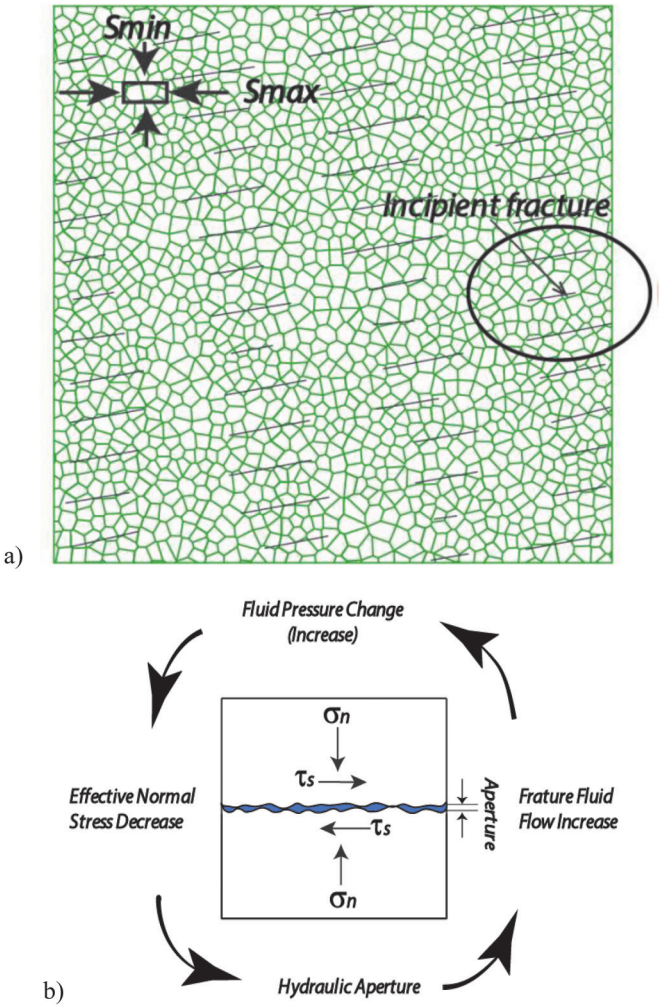

of the interactions between the natural fracture network and hydraulic fracture as directed by the in situ stress field.

Key for simulating hydraulic fracturing, UDEC is capable of performing a fully coupled hydromechanical analysis to model fluid flow through a network of fractures. Mechanical deformation of joint apertures changes conductivity and, conversely, the connectivity changes the joint water pressure, which affects the mechanical computations of joint aperture (Fig. 2). The blocks in this assemblage are treated as being impermeable. The cubic law for flow within a planar fracture is used, where the flow rate q is given by

$$q = ka^3\frac{\Delta P}{l} \quad (1)$$

where k is joint permeability, a is the contact hydraulic aperture, ΔP is the pressure difference between the two adjacent domains, and l is the length assigned to the contact between the domains. Because the UDEC formulation is restricted to modeling fracture flow, leak-off along the fractures diffusing into the rock matrix is assumed to be zero. (Only leak-off into incipient fractures is considered.) Furthermore, the fracture flow is idealized by means of a parallel plate model and cubic law, which disregards tortuosity.

Fig. 3. Rock mass model with background incipient fractures only, generated using Voronoi tessellation (20 m × 20 m).

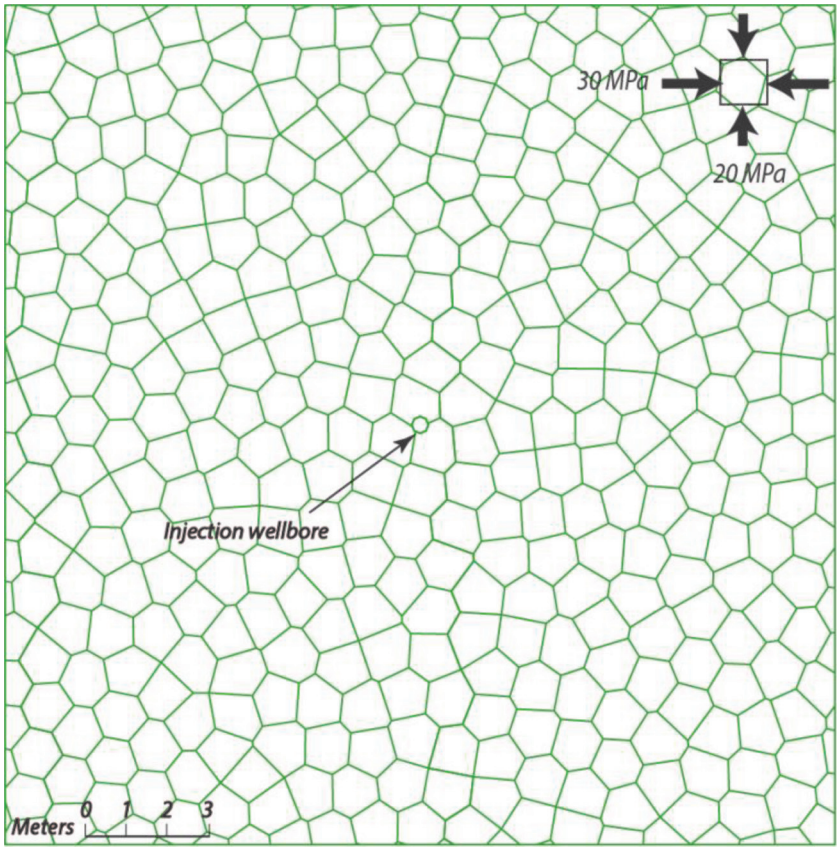

When a joint contact is broken, the fluid flows into the joint with a finite permeability k:

$$k = \frac{1}{12\mu} \quad (2)$$

where μ is fluid dynamic viscosity. The hydromechanical coupling is completed by associating the hydraulic aperture to the mechanical joint stiffness and acting effective normal stresses (i.e., mechanical aperture).

Influence of natural fractures in hydraulic fractures

Hubbert and Willis (1957) showed that hydraulic fractures in an isotropic medium always propagate perpendicular to the orientation of the minimum principal stress. In other words, the fracture propagates in the direction for which opening is most easily accommodated, propagating parallel to the maximum stress so that opening is against the minimum principal stress. However, in a nonisotropic medium, hydraulic fracturing mine-back experiments by Warren and Smith (1985) have shown that pre-existing fractures and faults can influence fracture propagation, although the overall trajectory is still controlled by the orientation of the minimum principal stress, as also noted by Zoback (2007).

Blanton (1982, 1986) studied how hydraulic fractures interact with natural fracture systems under different angles of approach and applied triaxial stress fields in a series of laboratory experiments on Devonian shale as well as blocks of pre-fractured hydrostone (cemented crushed rock). These experiments showed three classes of induced hydraulic fracture behaviour whereby the propagating fracture: (*i*) crosses the pre-existing fracture, (*ii*) is diverted by the pre-existing fracture, or (*iii*) is arrested by the pre-existing fracture. The behaviour was found to depend on the background stress conditions and the angle of approach to the pre-existing fracture.

Table 1. Model properties assigned.

Discontinuity property	Incipient fractures	Natural fractures
Friction angle (°)	30	25
Residual friction angle (°)	25	20
Cohesion (MPa)	1.0	0.0
Residual cohesion (MPa)	0.0	0.0
Tensile strength (MPa)	0.5	0.0
Residual tensile strength (MPa)	0.0	0.0
Normal stiffness (MPa/m)	1×10^4	1×10^3
Shear stiffness (MPa/m)	1×10^3	1×10^2

Warpinski and Teufel (1987) investigated the influence of geological discontinuities on the propagation of hydraulic fractures observed in mine-back experiments. They likewise confirmed that the geological discontinuities influence the overall geometry and effectiveness of the hydraulic fracture. They also showed that when a hydraulic fracture intersects a natural fracture or other discontinuity at some angle with respect to the hydraulic fracture (or the direction of maximum stress), the fracture will propagate across the natural fracture or activate and dilate the natural fracture in shear.

Olson et al. (2012) examined and showed the effects of cemented (or healed) natural fractures, under different angles of approach to the hydraulic fracture direction. These tests were done in a series of laboratory experiments on cast hydrostone containing embedded planar glass discontinuities as proxies for cemented natural fractures. These experiments showed that the induced hydraulic fracture can bypass the natural fracture by propagating

Fig. 4. Increased fracture aperture showing simulated hydraulic fracture initiation pattern for a reservoir rock composed of incipient fractures only.

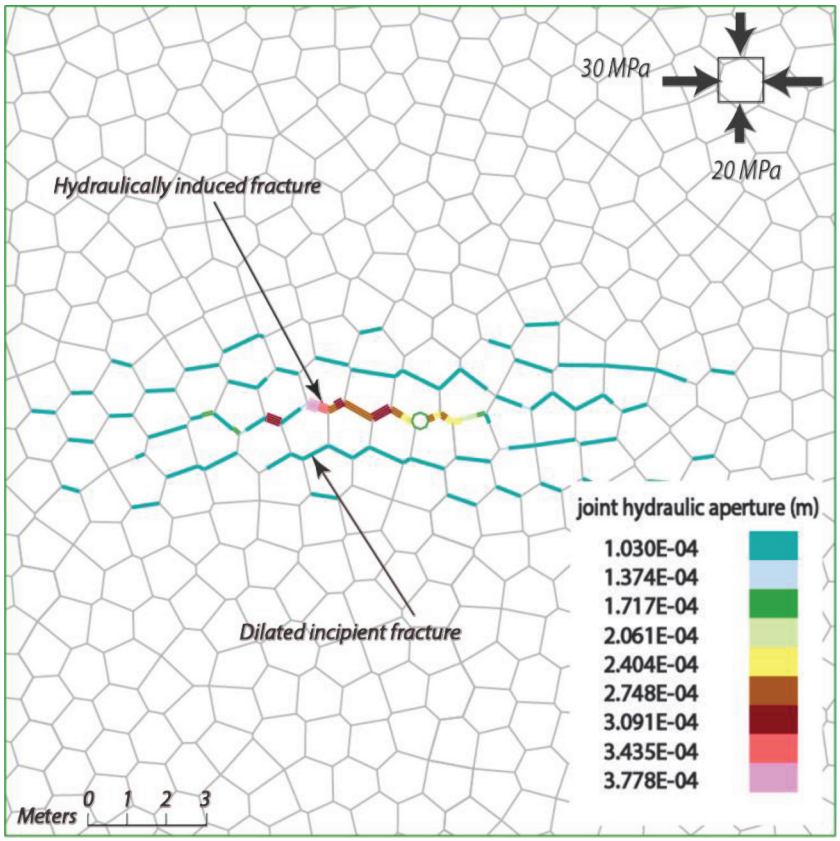

Fig. 5. Conceptualization (plan view) of the invaded and dilated zones (after Dusseault et al. 2011).

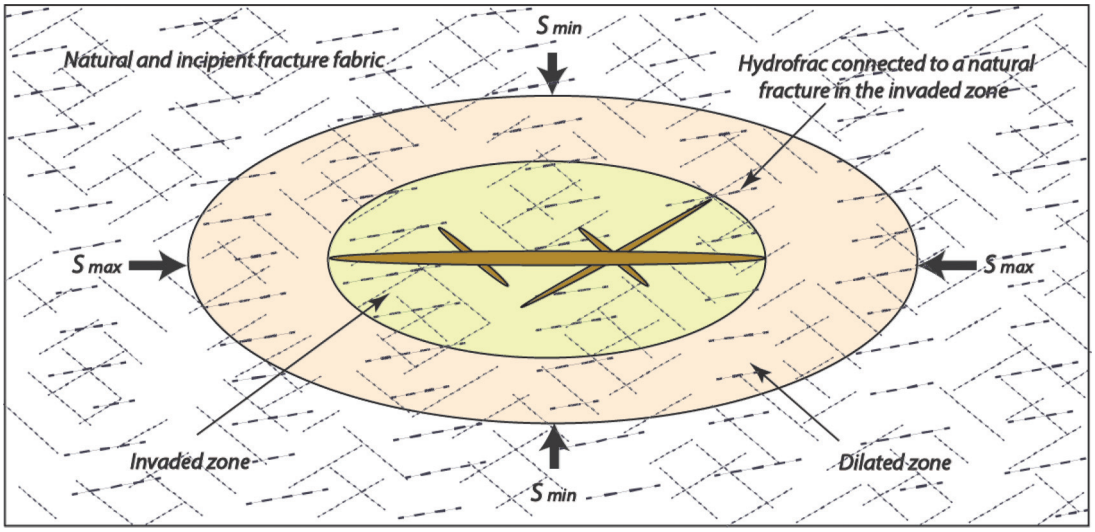

around it, be arrested by it or diverted along it, or undergo a combination of bypass and diversion.

Dershowitz et al. (2010) noted the significance of the interaction of natural fractures with the propagating fracture based on discrete fracture network (DFN) realizations. They studied the influence of natural fractures on hydraulic fracture propagation in cases where the distributed natural fractures are close to or cross the path along which the hydraulic fracture propagation is to occur.

UDEC simulations

Model setup

The rock mass modeled in this study includes both natural fractures and incipient fractures, as defined by Dusseault et al. (2011). Construction of the UDEC models began with the generation of the incipient fractures using the Voronoi tessellation generator (Fig. 3). The concept of incipient fractures is utilized to emphasize that not only are clearly visible fractures, identifiable in televiewer and core logs, opened or sheared, but incipient

Fig. 6. Simulated pore pressure distribution around the injection borehole.

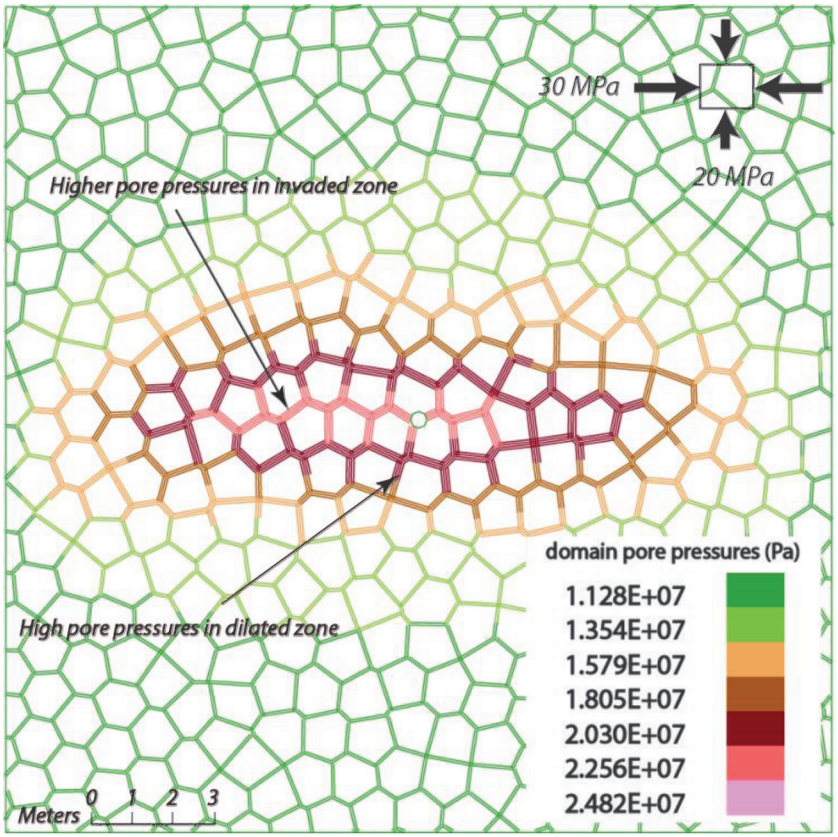

Fig. 7. Joints that open in response to the modeled hydraulic fracture (zero normal stress), shown in green, and fractures that shear and dilate in response to the change in the effective stresses, shown in red. ("Green" and "red" refer to Web version of this figure.)

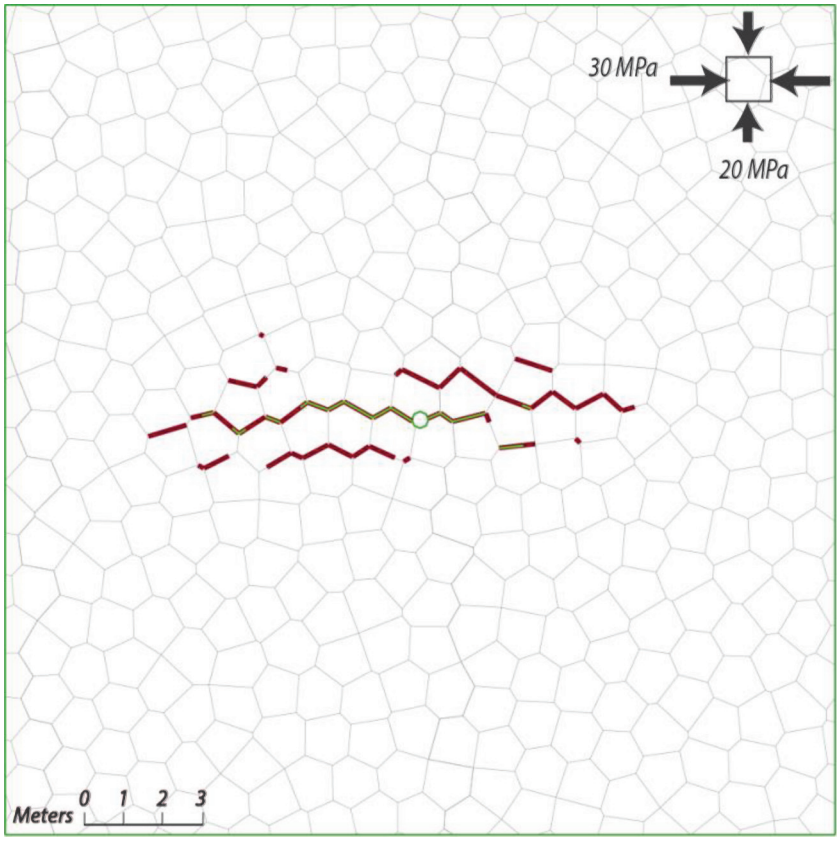

Fig. 8. Displacement vectors around the pressurized borehole.

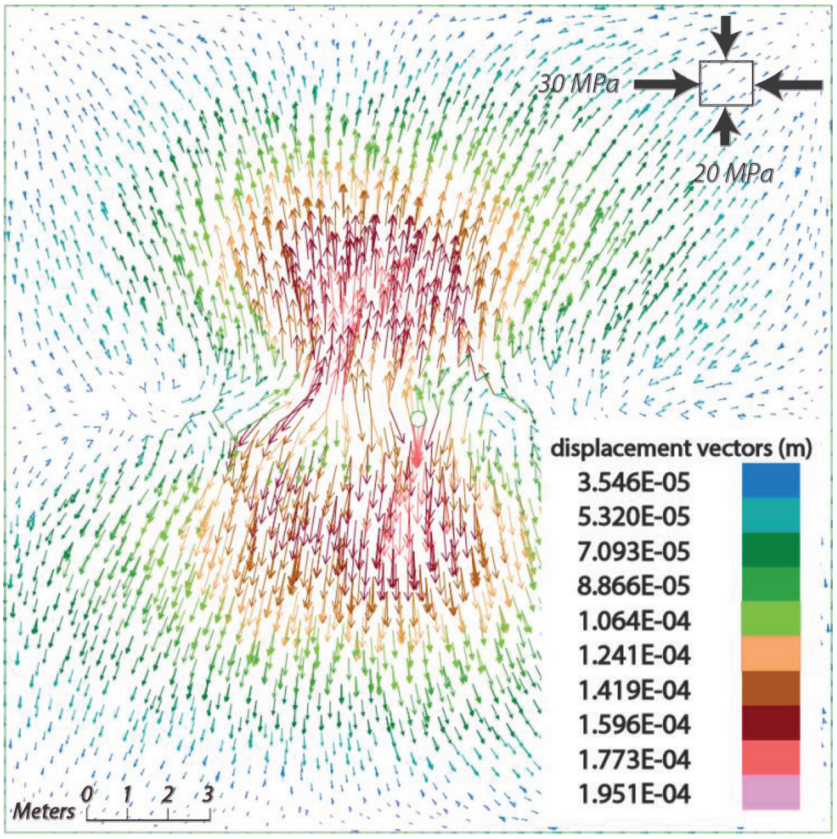

Fig. 9. Rock mass model including background incipient fractures transected by a persistent fault.

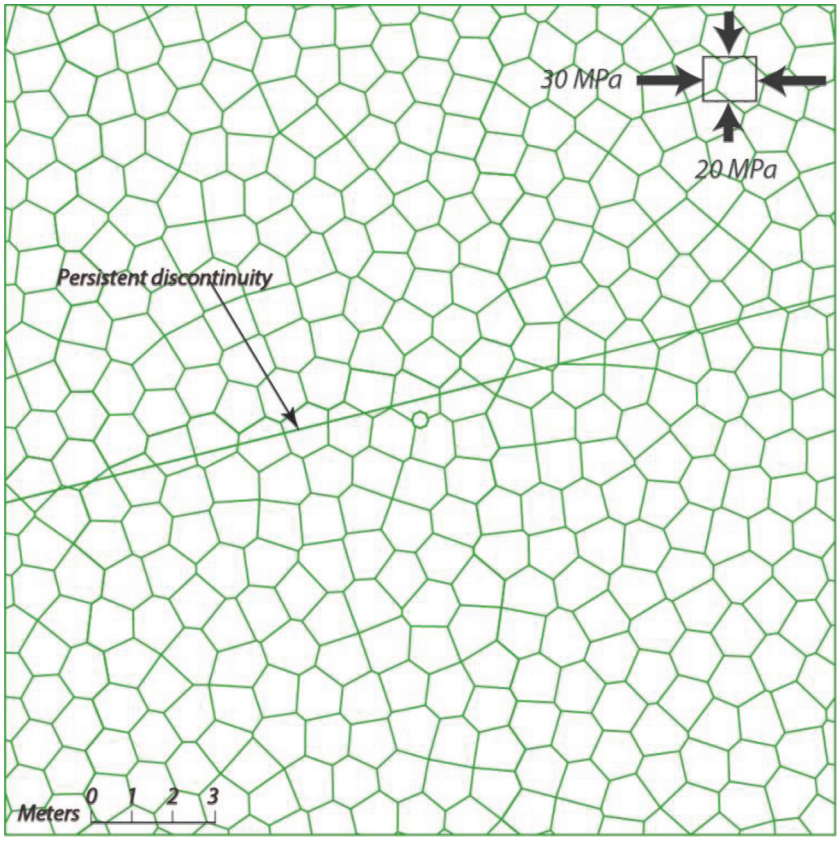

Fig. 10. Displacement vectors around the pressurized borehole and along the fault.

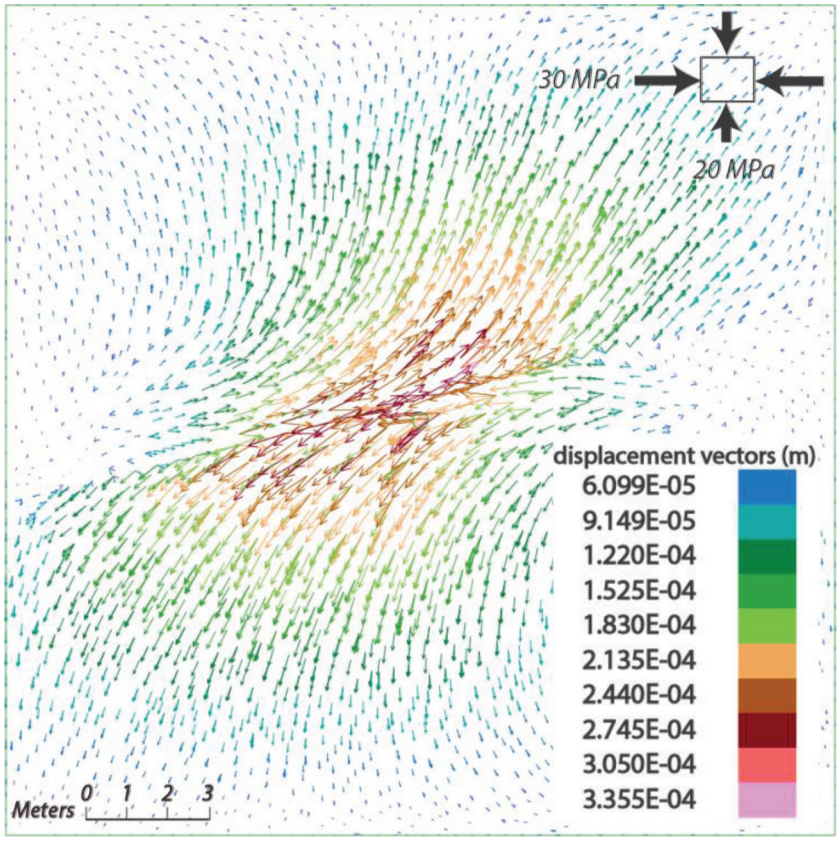

Fig. 11. Corresponding shear displacement along the fault in response to effective stress change.

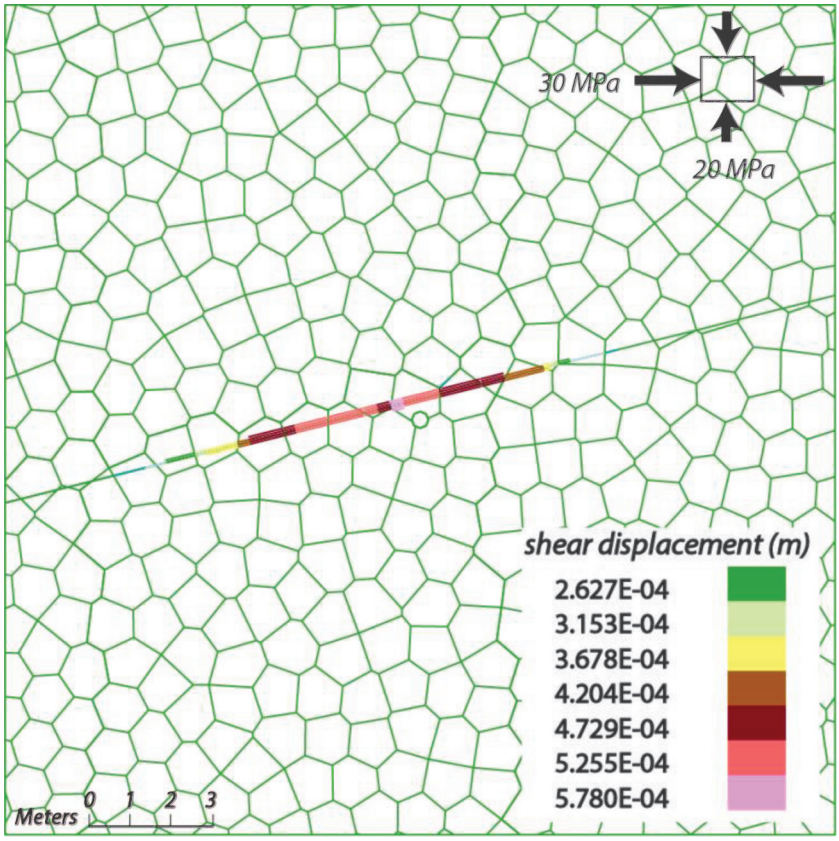

fractures can also serve as potential pathways for hydraulic fracture propagation. The embedded network of nonpersistent natural fractures were assigned zero cohesion and tensile strengths; the background network of incipient fractures were assigned the cohesion and tensile strengths reported in Table 1. Properties were approximately based on those derived from laboratory testing of reservoir rocks from northeastern British Columbia, with fracture stiffness values being assigned based on guidelines provided by the UDEC manual (Itasca Consulting Group 2011) and those reported by Zangerl et al. (2008).

Initial aperture values of 0.01 mm were assumed for the incipient fractures and 0.1 mm for the natural fractures. Variations in aperture in response to fluid pressure and normal stress changes are assumed to follow a linear relationship described by the normal stiffness (see Table 1). The incipient planes of weakness were modeled assuming a Coulomb-slip constitutive model with both peak and post-peak properties; these are given in Table 1. The blocks were modeled as being elastic with a Young's modulus of 30 GPa and a Poisson's ratio of 0.25.

The model (Fig. 3) represents a 2-D vertical plane, where the out-of-plane stress is horizontal. The vertical stress (σ_V) was assumed to align with the minimum principal stress (S_{min} or σ_3) and was set to 20 MPa; the out-of-plane horizontal stress (σ_2) was also set to 20 MPa. The maximum principal stress (S_{max} or σ_1) was assumed to be horizontal and parallel to the 2-D model section and was set to 30 MPa. The gravitational variation of vertical stress from top to bottom of the model is neglected because the variation is small in comparison with the magnitude of stress being modeled. An initial background pore pressure of 10 MPa was applied. The wellbores at the center of the model are pressurized with an incompressible slickwater fracturing fluid with no proppant. The wellbores pressurized in the model are horizontal and parallel to the out-of-plane direction (Fig. 2). Boundary conditions are specified for the external boundaries of the model, assuming constant stress and constant fluid pressure conditions.

Baseline case: Invaded and dilated zones

Figure 4 shows the simulation results of the baseline case involving fluid injection and hydraulic fracturing without the presence of natural fractures (as shown in Fig. 3). Fluid flow is accommodated along the network of incipient fractures. The results show the initiation and propagation of the hydraulic fracture in terms of increasing fracture aperture in response to fluid injection from the wellbore. Through the hydromechanical coupled logic used in UDEC, the stress field experiences local changes adjacent to the hydraulic fracture due to fracture opening.

The results in Fig. 4 also show an invaded zone adjacent to the hydraulic fracture, which represents an expanded zone of enhanced permeability. Dusseault et al. (2011) describe the development of an invaded and dilated zone during fluid injection, as shown in Fig. 5. They define the invaded zone as a region of propped fractures and the dilated zone as a region of naturally propped fractures opened by wedging, block rotation or shear dilation (Dusseault et al. 2011). The UDEC results can be seen to reproduce these zones in plots of the increased fracture aperture (Fig. 4), simulated pore pressure distribution (Fig. 6), and incipient fracture failure mode, which shows tensile opening along the path of the hydraulic fracture and shear slip and dilation in the surrounding invaded zone (Fig. 7). The simulated hydraulic fracture in Fig. 4 and pore pressure distribution in Fig. 6 show the dilated zone has enhanced flow properties.

Figure 8 shows the displacement vectors corresponding to the pressurized wellbore and induced hydraulic fracture. The displacement vectors indicate that the main mode of deformation is fracture opening, with the incipient joints along the hydraulic fractures failing in tension. A different response is observed when a persistent discontinuity — for example, a fault — is added to the rock mass near the wellbore. Figure 9 shows the model geometry

Fig. 12. Distinct-element rock mass model with distributed natural fractures. Zoomed-in window provided above.

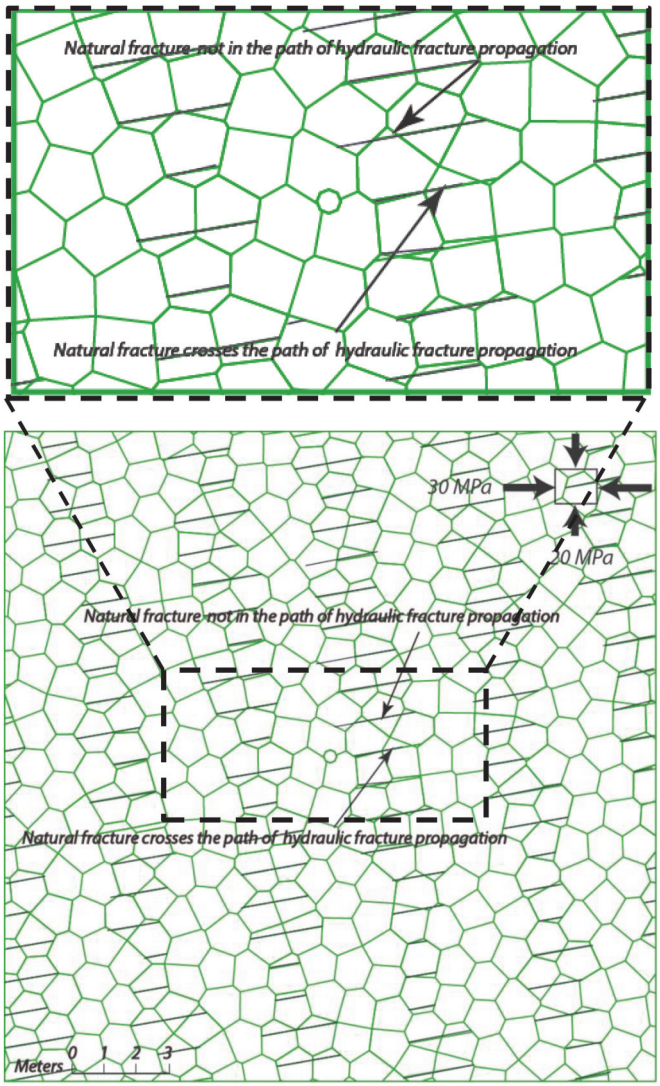

for this scenario, with properties for the fault provided in Table 1. The wellbore is pressurized and, as a result, a hydraulic fracture is generated, which intersects the fault and induces slip along the fault (Fig. 10). Figure 11 shows the shear displacements along the fault, indicating that the main mode of deformation is shear dilation.

Influence of natural fractures on propagation of hydraulic fractures

As demonstrated in the previous section, the complexity of the hydraulic fracture and surrounding dilated zone depends on the presence of incipient and natural fractures populating the reservoir rock mass. These fractures are ubiquitous throughout the rock mass. To investigate the influence of natural fractures on propagation of hydraulic fractures more closely, UDEC was used to simulate the interactions between a propagating hydraulic fracture and a network of parallel, nonpersistent natural fractures which intersect or are near the hydraulic fracture propagation path (Fig. 12), as described by Dershowitz et al. (2010).

Figures 13 and 14 show that the induced hydraulic fracture propagates perpendicular to the minimum in situ stress and coalesces with one of the natural fractures as it propagates. Although the overall trajectory of the induced hydraulic fracture is

Fig. 13. Simulated pore pressure distribution showing influence of natural fractures on development of invaded and dilated zones.

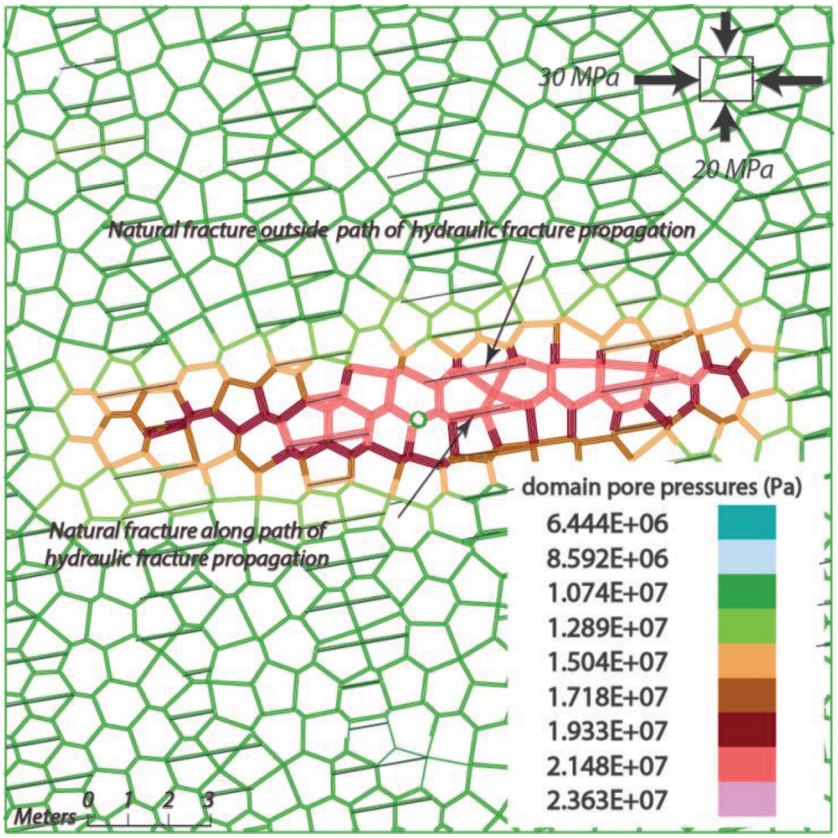

Fig. 14. Modeled apertures showing interactions that develop between induced hydraulic fracture and natural fractures, including development of invaded and dilated zones.

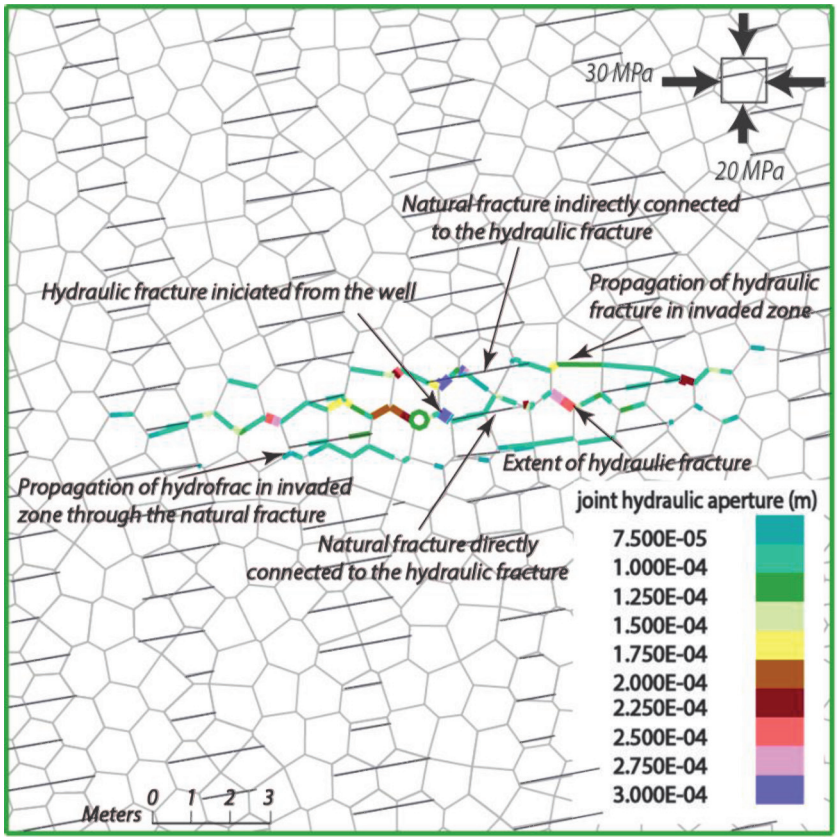

Fig. 15. Joints that open in response to modeled hydraulic fracture (zero normal stress), shown in green, and fractures that shear and dilate in response to change in effective stresses, shown in red. ("Green" and "red" refer to Web version of this figure.)

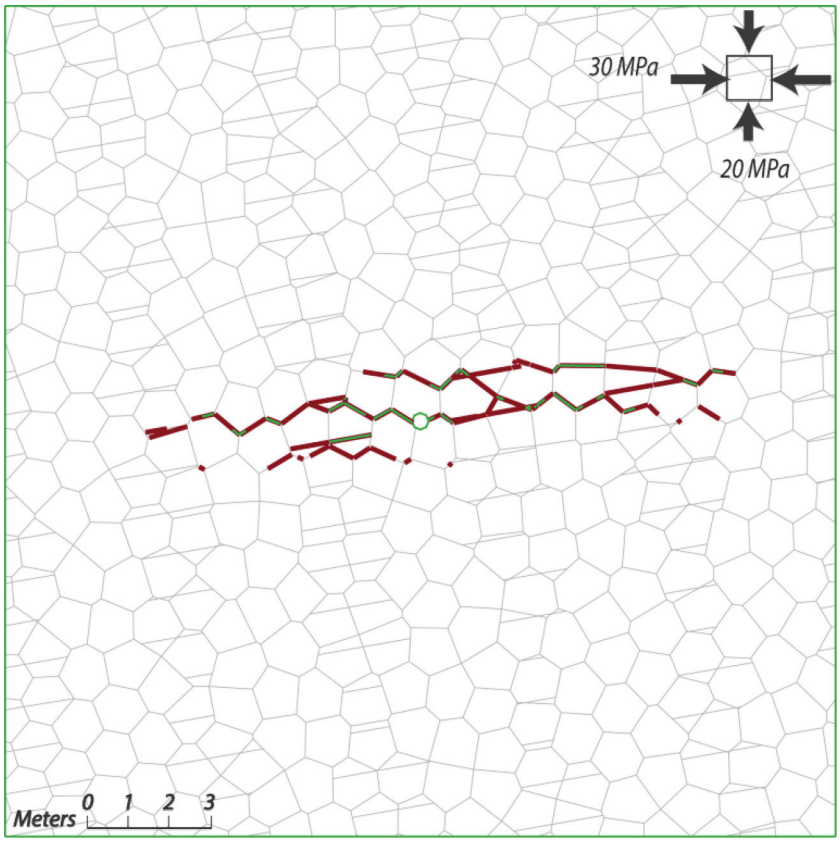

controlled by the in situ stresses, the natural fracture near the propagation path has an influence on the induced fracture. This effect is shown in the simulated pore pressure distribution (Fig. 13), which indicates an asymmetric response with higher pressures developing to the right of the wellbore where the hydraulic fracture path directly intersects a natural fracture. This natural fracture helps the hydraulic fracture advance (Fig. 14), diverting the injection fluid because of its lower resistance to aperture opening (i.e., higher hydraulic conductivity).

Further interrogation of the pore pressure distribution (Fig. 13) indicates that other natural fractures near the hydraulic fracture propagation path contribute to the development of the invaded and dilated zones (Fig. 14). Therefore, in addition to influencing the hydraulic fracture propagation path, natural fractures also influence the dilated zone (Fig. 15).

Effect of differential stress and angle of approach on interaction between hydraulic fracture and natural fractures

Blanton (1982, 1986) showed that the interaction of a hydraulic fracture with a natural fracture under different angles of approach (i.e., the angle between the propagating hydraulic fracture and natural fracture, as shown in Fig. 16) may result in one of three responses. First, if the injection pressures are sufficient, the hydraulic fracture may propagate across the natural fracture without changing direction, with the hydraulic fracture remaining essentially planar. The second scenario is where the hydraulic fracture does not cross the natural fracture but fluid pressures are sufficient to offset and initiate a continuation of the hydraulic fracture from the tip of the natural fracture. The third scenario is where the hydraulic fracture may stop propagating (arrest) after it approaches and intersects the natural fracture; in this case, the fluid pressure drops below that needed for the hydraulic fracture to continue, because of leak-off into the natural fracture. Whether the hydraulic fracture crosses or doesn't cross the natural fracture also depends on the in situ stress conditions relative to the orientation and properties of the natural fracture.

A series of UDEC experiments was carried out to investigate the types of interactions that can be expected between a hydraulic fracture and natural fracture for different ranges of approach angles and stress states. Table 2 summarizes the differential stress and approach angle under which each case was modeled.

Crossing interaction

An example where the UDEC simulation produced a hydraulic fracture that crossed a pre-existing natural fracture is shown in Fig. 17. In this case, the hydraulic fracture approaches the natural fracture with a high incidence angle of 60° under high differential in situ stresses ($\sigma_1 - \sigma_3 > 11$ MPa). The results presented in Figs. 18 and 19 show the induced hydraulic fracture (via incipient fractures that have opened) and simulated pore pressure distributions, respectively. The model suggests that the high angle of approach between the induced fracture and natural fracture results in a crossing interaction because the pressure required to redirect the hydraulic fracture and open in a direction nonparallel to the minimum in situ stress is greater than the pressure needed for the hydraulic fracture to continue along the same path as if the high-angled natural fracture were not there (despite the natural fracture being weaker than the incipient fractures). At the same time, the injection pressure is sufficient despite leak-off for the hydraulic fracture to continue propagating instead of arresting.

The induced hydraulic fracture in Fig. 18 indicates that it propagates as a bi-wing fracture, in both directions from the wellbore.

Fig. 16. Diagram of hydraulic fracture intersecting natural fracture.

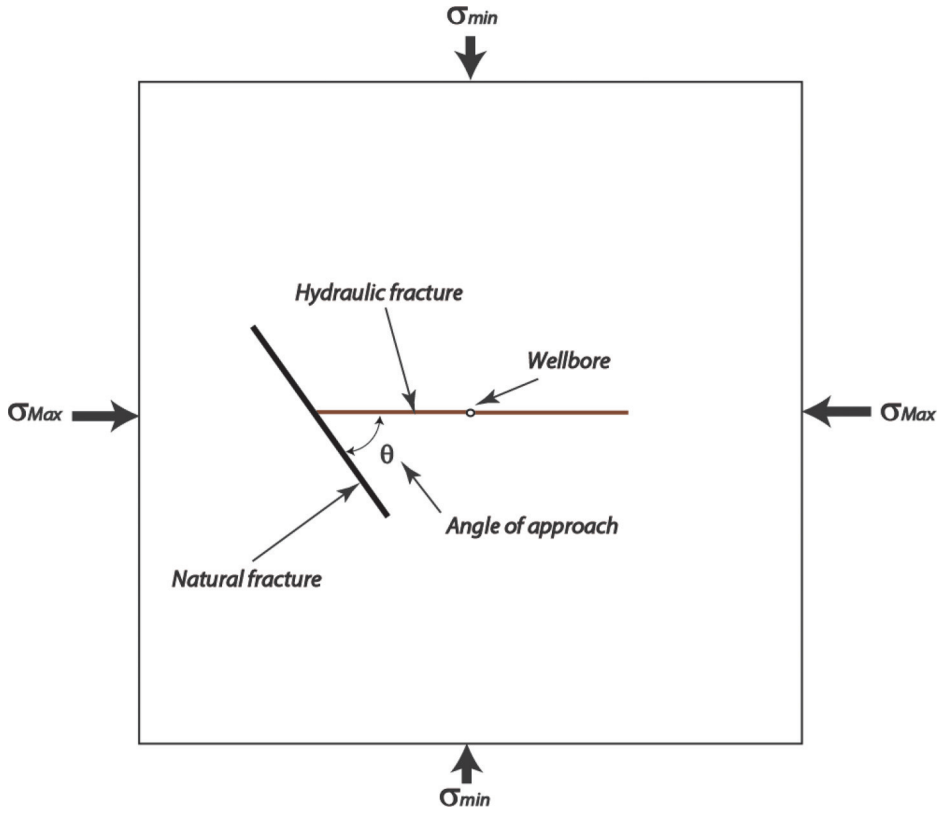

Table 2. Assigned in situ stress states and approach angles to investigate different hydraulic fracture responses to natural fracture intersections.

Interaction behavior	S_{max} (MPa)	S_{min} (MPa)	Differential stress (MPa)	Angle of approach (°)
Crossing	30	19	11	60
Offsetting	30	23	7	30
Arresting	30	21	9	45

Further interrogation of the pore pressure distribution (Fig. 19) likewise indicates a bi-wing pattern with pore pressures increasing on both sides of the wellbore. The tensile and opening response of the invaded zone to fluid injection is shown in Fig. 20.

Offset interaction

The second scenario, where a hydraulic fracture approaches, propagates along, and then resumes along an offset path from the tip of the natural fracture was observed when the approach angle was less than 30° and the differential in situ stresses was low (Fig. 21). The results presented in Figs. 22 and 23 show the induced fractures and simulated pore pressure distribution, respectively. The model suggests that the low angle of approach between the hydraulic fracture and natural fracture under a low in situ differential stress ($\sigma_1 - \sigma_3 < 7$ MPa) favored a path re-routed along the lower-strength natural fracture (zero cohesion and tensile strength) even though it was not optimally oriented with respect to the minimum principal stress. This scenario compares to the alternative propagation path along an incipient fracture more optimally oriented relative to the minimum principal stress, but with a finite cohesive and tensile strength. The approach angle was low enough in this case that the hydraulic fracture favored the weakest path.

The fracture pattern also suggests that the opening of the natural fracture limits the effectiveness of the hydraulic fracture as a result of the injected fluid being diverted to the natural fracture (i.e., leak-off). This diversion causes an offset in the hydraulic fracture propagation path and results in an asymmetric propagation response. This asymmetry can be seen in both the hydraulic fracture (Fig. 22) and pore pressure distribution (Fig. 23), with leak-off occurring into the natural fracture resulting in a localized increase in the dilated zone (Fig. 24).

Arresting interaction

The third scenario, involving an arresting response, were observed in the simulations when the hydraulic fracture approached the natural fracture with an angle of 45° under intermediate differential in situ stress conditions (Fig. 25). Results presented in Figs. 26 and 27, show the induced hydraulic fracture and simulated pore pressure distributions, respectively. The fracture pattern in Fig. 26 suggests that the 45° angle of approach is too sharp for the hydraulic fracture to cross but is not inclined at a suitable angle relative to the minimum principal stress for the fluid pressures to open the natural fracture and allow the hydraulic fracture to continue propagating from the crack tip of the natural fracture (i.e., offset interaction).

The result is that the arresting of the hydraulic fracture significantly limits the effectiveness of the treatment. Figure 27 shows that the propagation of the hydraulic fracture is asymmetric, as a result of the arrested interaction; a continuum analysis would inherently predict a symmetric hydraulic fracture around the wellbore. Further interrogation of the pore pressure distribution (Fig. 27) indicates higher pore pressure increase around the wellbore in the dilated zone, which ultimately could cause the hydraulic fracture to branch and grow in that zone. The tensile and opening response of the model to fluid injection is shown in Fig. 28. The branching would be facilitated by the presence of the ubiquitous natural fracture network, as shown in Fig. 14.

In this case, hydraulic fracture arrest occurred under intermediate differential stresses ($\sigma_1 - \sigma_3 \approx 9$ MPa) and at an intermediate

Fig. 17. Rock mass model (200 m × 200 m) with background of incipient fractures superimposed with a natural fracture at a 60° angle of approach.

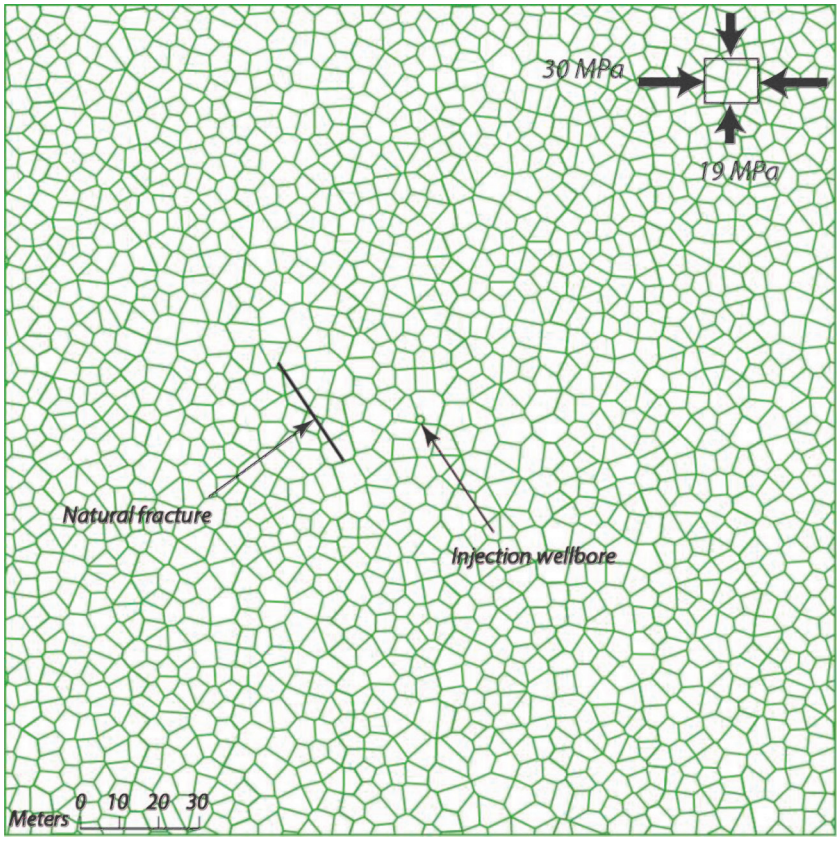

Fig. 18. Modeled response of the induced hydraulic fracture (i.e., incipient fractures that have opened) as it intersects a natural fracture at a 60° approach angle under high differential stresses. In this case the hydraulic fracture crosses the natural fracture.

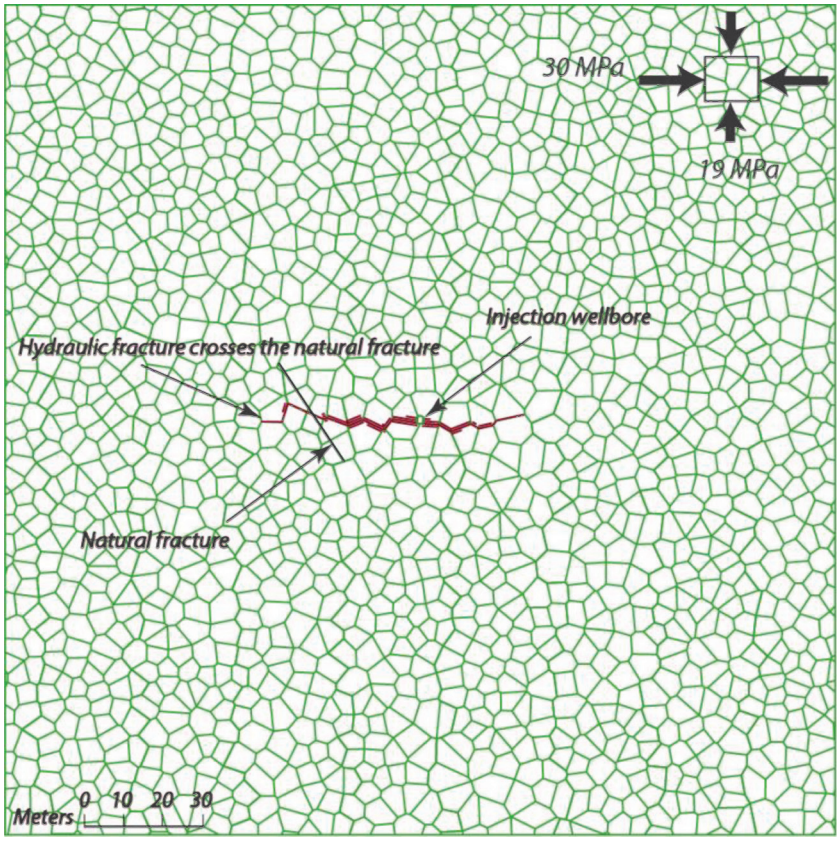

Fig. 19. Simulated pore pressure distribution for scenario assuming a natural fracture at a 60° approach angle under high differential stresses.

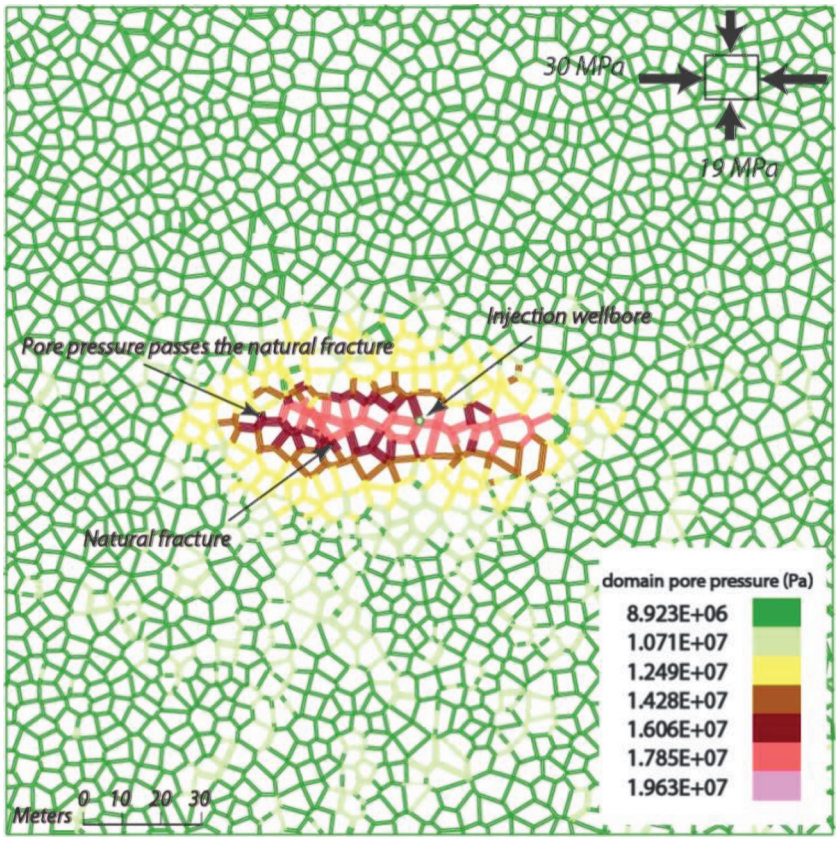

Fig. 20. Joints that open in response to the modeled hydraulic fracture (zero normal stress), shown in green, and fractures that shear and dilate in response to the change in the effective stresses, shown in red. ("Green" and "red" refer to Web version of this figure.)

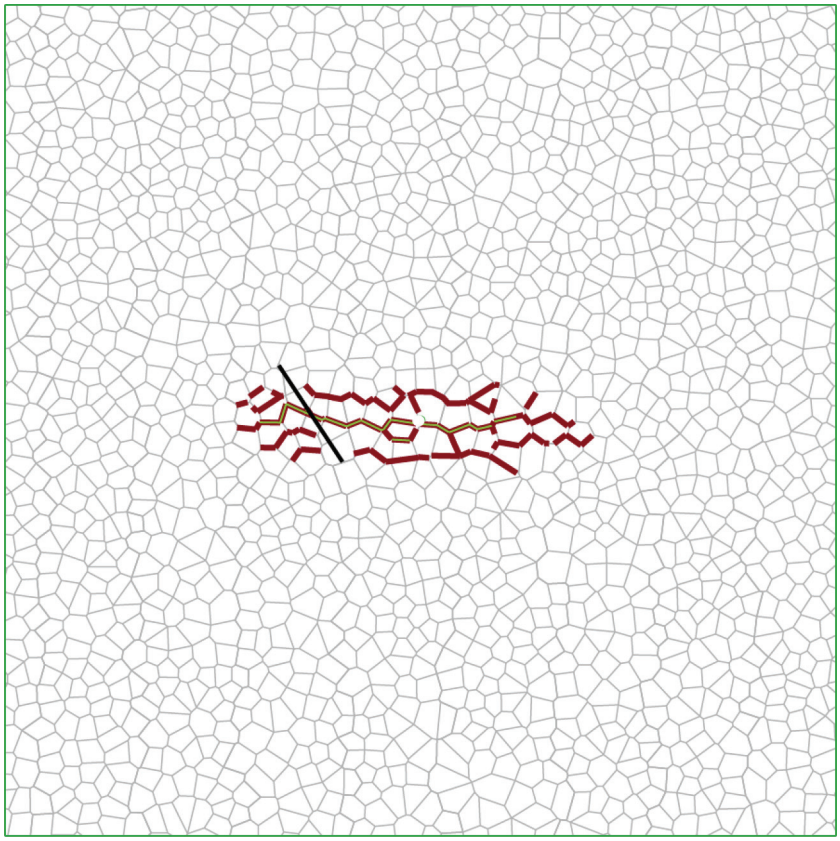

Fig. 21. Rock mass model (200 m × 200 m) with background of incipient fractures superimposed with a natural fracture at a 30° angle of approach.

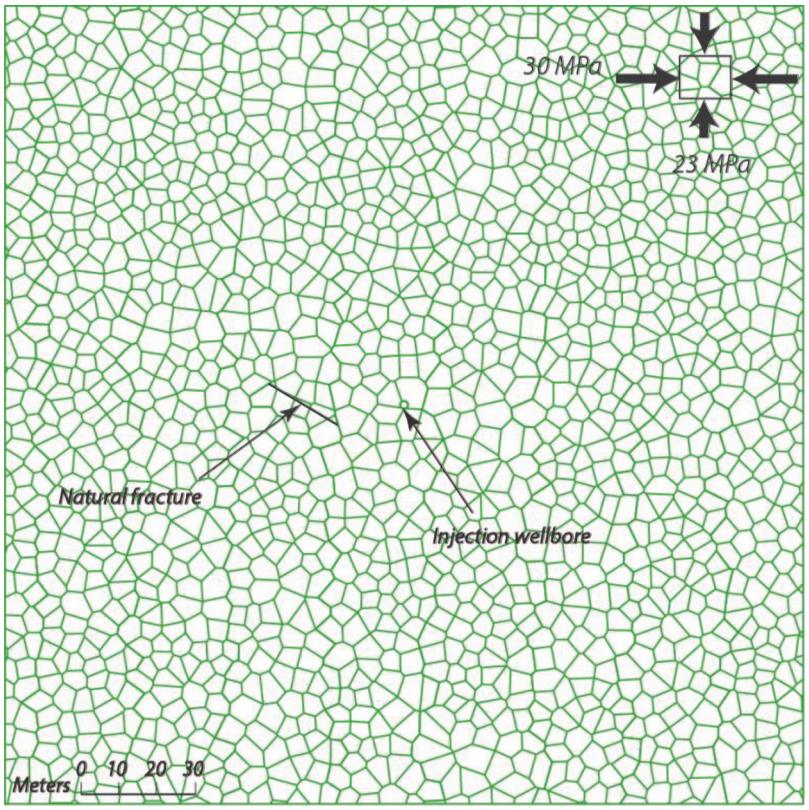

Fig. 22. Modeled response of the induced hydraulic fracture as it intersects a natural fracture at a 30° approach angle under low differential stresses. In this case the hydraulic fracture path is offset by the natural fracture.

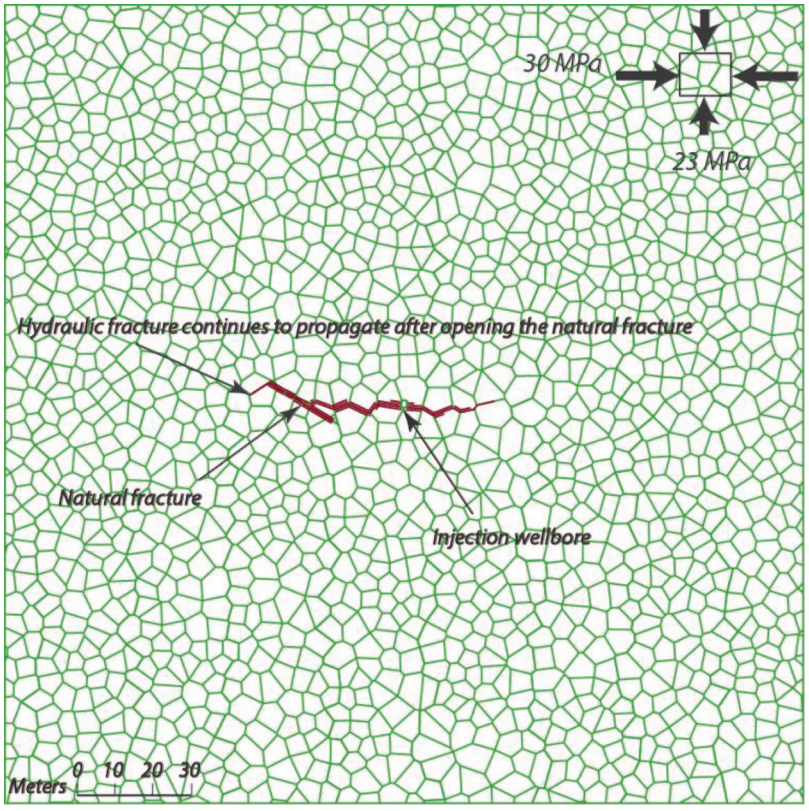

Fig. 23. Simulated pore pressure distribution for scenario assuming a natural fracture at a 30° approach angle under low differential stresses.

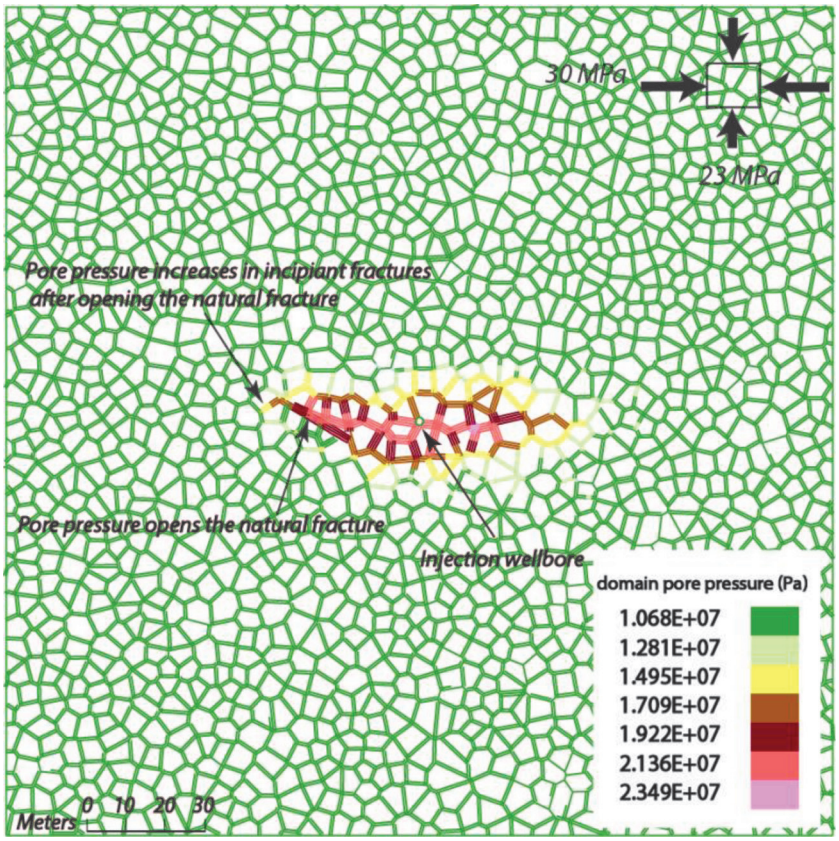

Fig. 24. Joints that open in response to modeled hydraulic fracture (zero normal stress), shown in green, and fractures that shear and dilate in response to change in effective stresses, shown in red. ("Green" and "red" refer to Web version of this figure.)

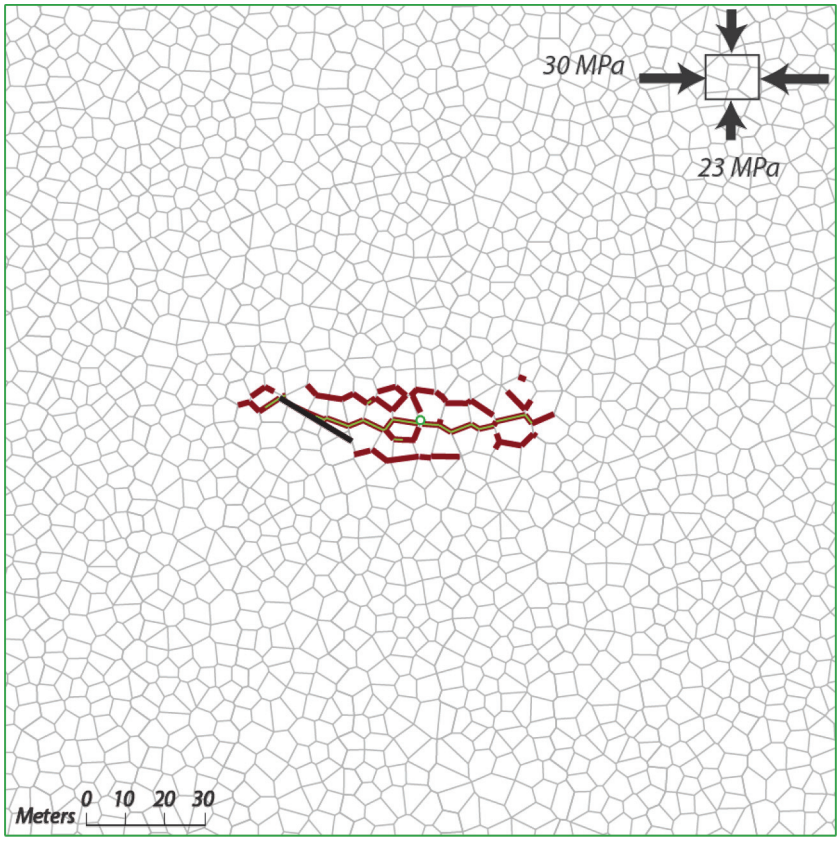

Fig. 25. Rock mass model (200 m × 200 m) with background of incipient fractures superimposed with a natural fracture at a 45° angle of approach.

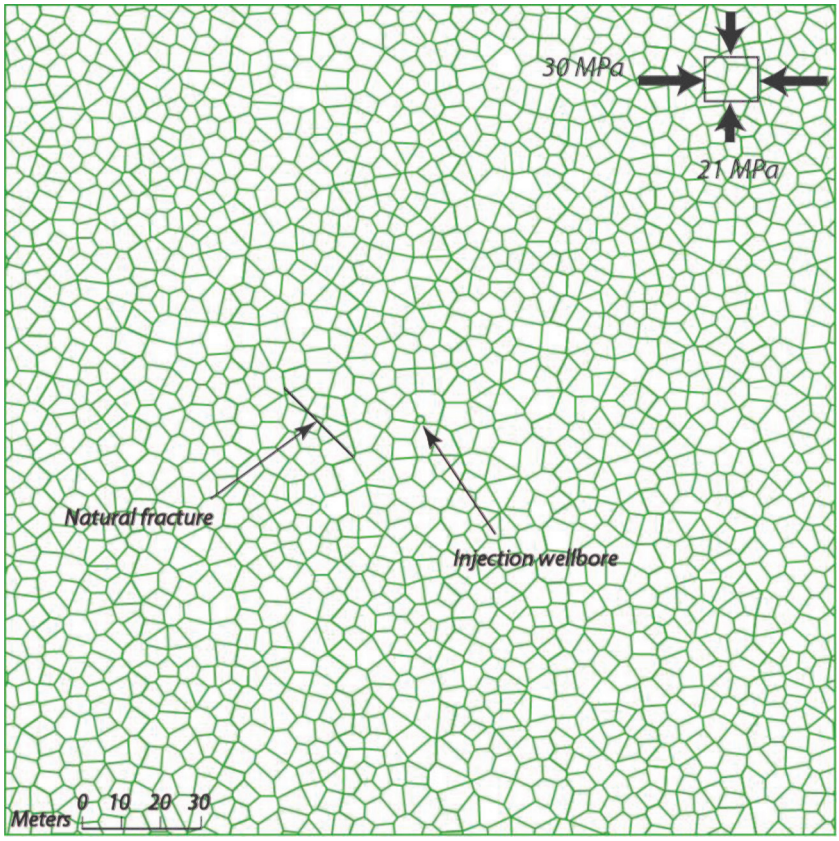

Fig. 26. Modeled response of the induced hydraulic fracture as it intersects a natural fracture at a 45° approach angle under intermediate differential stresses. In this case the hydraulic fracture is stopped by the natural fracture.

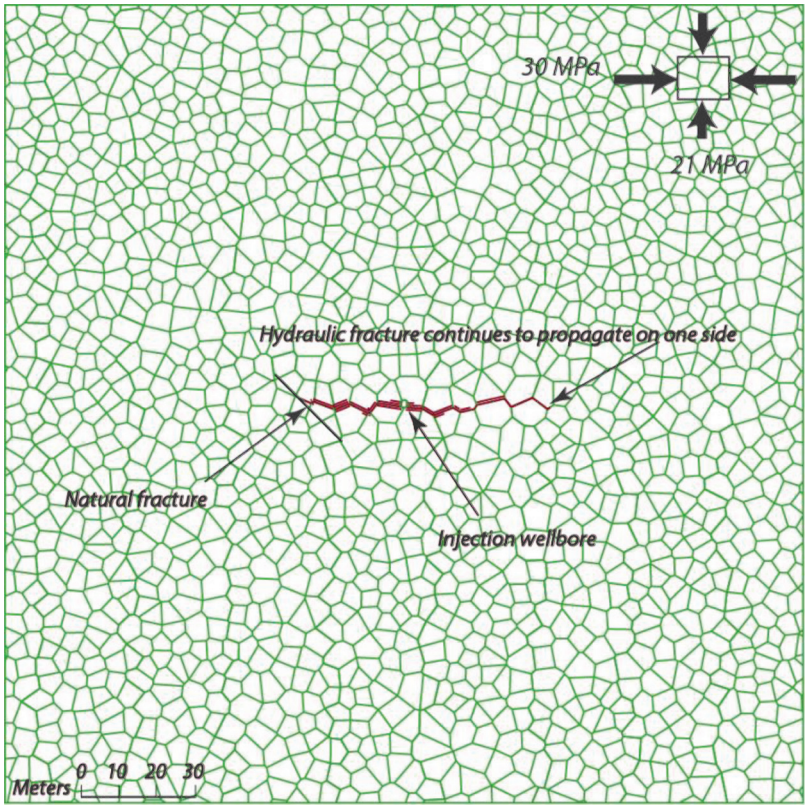

Fig. 27. Simulated pore pressure distribution for scenario assuming a natural fracture at a 45° approach angle under intermediate differential stresses.

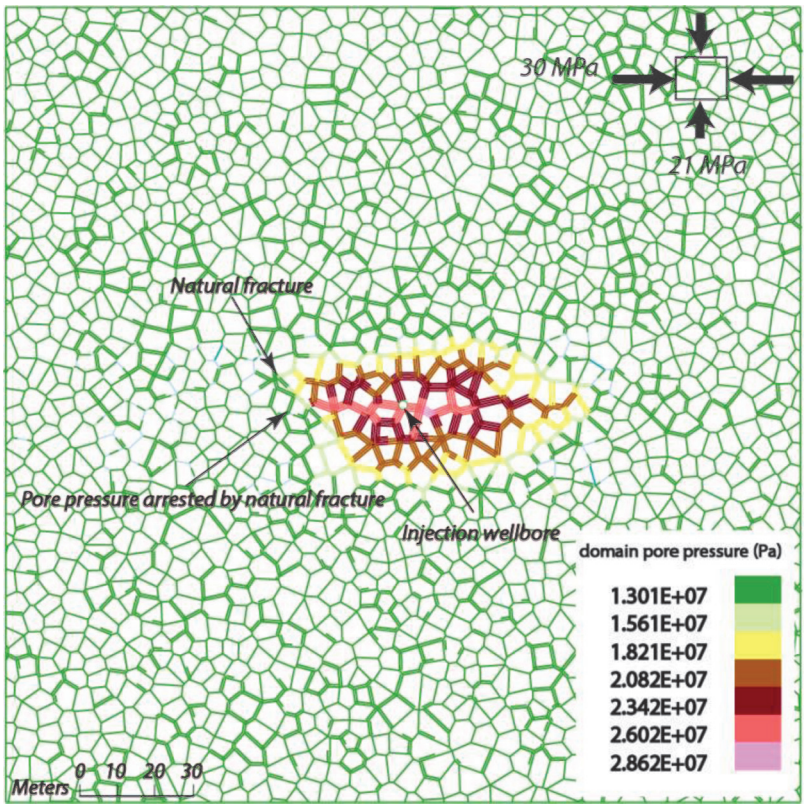

Fig. 28. Joints that open in response to modeled hydraulic fracture (zero normal stress), shown in green, and fractures that shear and dilate in response to change in effective stresses, shown in red. ("Green" and "red" refer to Web version of this figure.)

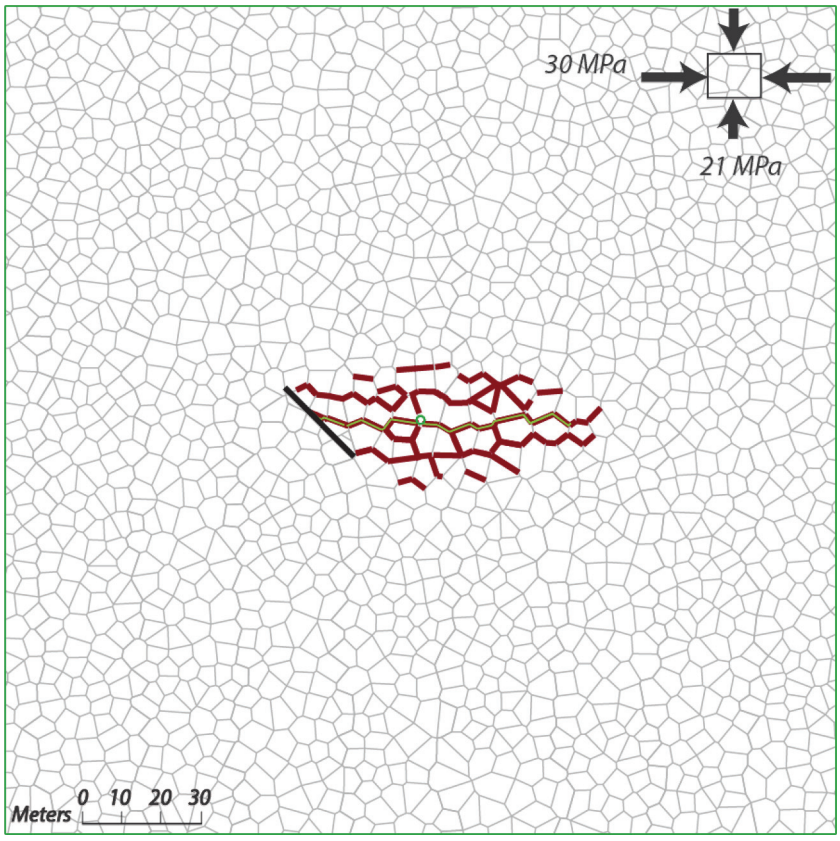

Fig. 29. Correlation between angle of approach and differential stress, based on UDEC-based numerical experiments.

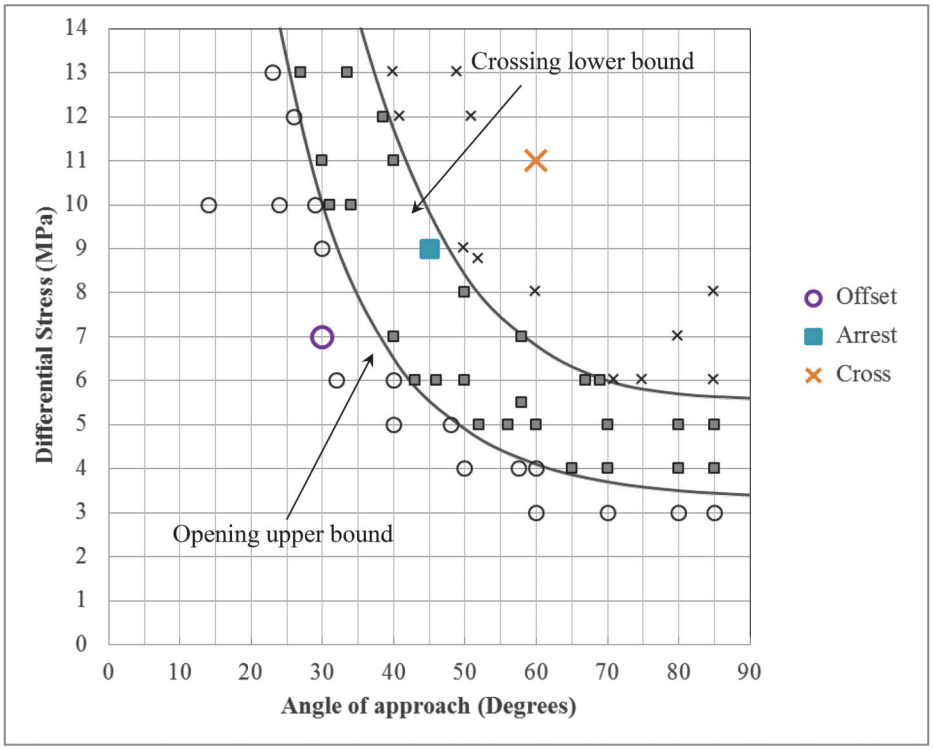

angle of approach (45°). Arresting could be a temporary interaction response, and, through continued pressure increase, offset or crossing may be advanced. When the injection pressure exceeds the normal stress acting across the natural fracture (i.e., zero effective normal stress), the natural fracture will open, slip, and dilate, and fluid pressure will leak off into the natural fracture. With continued injection, the hydraulic fracture may then reinitiate once the pressure required to open the adjacent incipient fractures is exceeded. This staged interaction results in significant asymmetry in the hydraulic fracture length, relative to the two sides initiated from the wellbore, as well as with respect to the degree of hydraulic fracture branching in the dilated zone.

Bounding relationships as a function of approach angle and stress state

Based on the scenarios described in the previous section, a series of sensitivity analyses were performed to provide a basis for selecting fracturing treatments that are most effective in connecting the natural fracture network to the wellbore and hydraulic fracture. Figure 29 shows the results of a series of numerical experiments applying several different angles of approach and states of stress using the bisection approach, which is a variation of the incremental search method (Chopra 2008). The results show clear zones of opening- and crossing-type interactions, separated by a zone of arresting interaction between the opening and crossing limits. The type-cases representing the three scenarios described in the previous sections are highlighted in Fig. 29. The UDEC results for each point presented in Fig. 29 are provided in Zangeneh (2013).

The analyses carried out here were based on a conceptualized model of a shale gas reservoir. The same numerical study can be performed for any given reservoir to determine site-specific correlations between the planned hydraulic fracture and natural fracture sets, together with the in situ stress conditions present in the basin under study. The numerical modeling procedure outlined here would provide a valuable tool for decision makers to assess the potential for crossing, offsetting or arresting interactions, and the potential for asymmetric hydraulic fracturing treatments.

Conclusions

Distinct-element numerical modeling techniques have been investigated for their ability to model the interactions between a hydraulic fracture and a network of natural fractures. The discontinuum-based approach showed value in modeling the complex behavior of hydraulic fracture propagation in a naturally fractured reservoir. The model was capable of simulating the tensile failure and shear dilation of incipient fractures in the intact rock and along reactivated natural fractures. Furthermore, the models were also able to simulate the interconnections that develop adjacent to the hydraulic fracture in the invaded and dilated zones. The value of using a discontinuum- over a continuum-based approach was demonstrated through its ability to model asymmetric hydraulic fracture behaviors in response to the presence of natural fractures. The importance of accounting for natural fractures in the invaded zone was investigated, and the results show a considerable influence with respect to enhanced permeability arising from branching and dilation of fractures adjacent to the propagating hydraulic fracture.

Interactions between the induced hydraulic fracture and existing natural fractures were further examined with respect to different approach angles and in situ stress states. The numerical results showed that hydraulic fractures tend to cross pre-existing natural fractures under high differential stresses and high angles of approach. At low differential stresses and angles of approach, natural fractures tend to open and divert injected fluids, resulting in a re-routing of the hydraulic fracture such that it offsets and re-initiates, propagating from the tip of the natural fracture. An intermediate differential stress and angle of approach was seen to result in the arrest (i.e., stoppage) of the hydraulic fracture propagation.

The implication of this study for hydraulic fracturing designs is that the orientation of the fracture network relative to that of the in situ stress field plays an important role with respect to the extent and symmetry of hydraulic fracture propagation, and thus the overall success of achieving the reservoir coverage desired. Symmetric fracture extension on both sides of a wellbore is unlikely in the presence of a larger discrete fracture such as a fault, because of the different stress and coupled hydromechanical interactions that arise. Exceptions may arise where high differential stresses and a high angle of approach results in the hydraulic fracture crossing natural fractures in its path. The presence of natural fractures may further act to redirect fluid pressures, requiring longer pressurization intervals to achieve the desirable fracture length, with consideration given to pressure and fluid leak-off into adjacent natural fractures. In the worst-case scenario, the presence of an adversely oriented natural fracture (under intermediate differential stresses and intermediate angle of approach) may cause the hydraulic fracture propagation to stop. As a result, a longer pressurization or higher pumping pressures may be required to re-initiate the hydraulic fracture to achieve the desirable fracture length.

In different parts of a basin, the dominant fracture network angle could spatially vary (e.g., Appalachian Basin; see Cliffs Minerals Inc. 1982). As a result, different interactions can be expected across different zones in the basin. This variation introduces an impact on the effectiveness of hydraulic fracturing treatment; the orientation of the natural fractures relative to the stress field could adversely affect the propagation of the hydraulic fracture, possibly limiting its extension beyond the first set of natural fractures it encounters. The extension of connection between wellbore and natural fractures can be achieved by further pumping, which may be of value in some reservoir treatments (Blanton 1986). Therefore, in different zones of a basin, different decisions may be required regarding operational factors based on an understanding of the type of potential interactions that may develop between the hydraulic fracture and natural fractures.

The purpose of this study was to provide a conceptual basis for selecting fracturing treatments that will result in an effective connection between a hydraulic fracture, natural fracture network, and injection wellbore. Future work will involve applying these techniques to an actual gas shale reservoir and ground-truthing the modeling results using field data (e.g., microseismic monitoring data). Future work will also involve (*i*) closely examinating other parameters, such as the properties of the natural fractures and their variability; (*ii*) investigating other limiting assumptions such as the role of fluid viscosity, natural fracture aperture, tortuosity, the use of proppant; and (*iii*) extending the models to three dimensions.

Acknowledgements

The authors would like to thank the Natural Sciences and Engineering Research Council of Canada (NSERC), Trican Well Service Ltd., Geoscience B.C., and the B.C. Oil and Gas Commission for their financial support of this work.

References

Barree, R.D. 1983. A particular numerical simulator for three-dimensional fracture propagation in heterogeneous media. Society of Petroleum Engineers. SPE 12273. doi:10.2118/12273-MS.

Blanton, T.L. 1982. An experimental study of interaction between hydraulically induced and pre-existing fractures. Society of Petroleum Engineers. SPE/DOE 10847. doi:10.2118/10847-MS.

Blanton, T.L. 1986. Propagation of hydraulically and dynamically induced fractures in naturally fractured reservoirs. Society of Petroleum Engineers. SPE 15261. doi:10.2118/15261-MS.

Choi, S.O. 2012. Interpretation of shut-in pressure in hydrofracturing pressure-time records using numerical modeling. International Journal of Rock Mechanics and Mining Sciences, **50**: 29–37. doi:10.1016/j.ijrmms.2011.12.001.

Chopra, S.C. 2008. Applied numerical methods with MATLAB. 2nd ed. McGraw Hill.

Cleary, M.P. 1980. Comprehensive design formulae for hydraulic fracturing. Society of Petroleum Engineers, SPE 9259. doi:10.2118/9259-MS.

Cleary, M.P., Wright, C.A. and Wright, T.S. 1991. Experimental and modeling evidence for major changes in hydraulic fracturing design and field procedures. Society of Petroleum Engineers, SPE 21494. doi:10.2118/21494-MS.

Cliff Minerals Inc. 1982. Analysis of the Devonian shale in the Appalachian basin: Final report to US Department of Energy under contract DE-AC21-80MC14693, V.1 and 2, Morgantown W.Va.

Cundall, P.A., and Hart, R.D. 1992. Numerical modelling of discontinua. Engineering Computations, **9**: 101–113. doi:10.1108/eb023851.

Damjanac, B., Gil, I., Pierce, M., Sanchez, M., Van As, A., and McLennan, J. 2010. A new approach to hydraulic fracturing modeling in naturally fractured reservoirs. *In* Proceeedings of the 44th U.S. Rock Mechanics Symposium and 5th U.S.-Canada Rock Mechanics Symposium, 2010, Salt Lake City, Utah, June 27–30. ARMA 10-400.

Dershowitz, W.S., Cottrell, M.G., Lim, D.H., and, Doe, T.W. 2010. A discrete fracture network approach for evaluation of hydraulic fracture stimulation of naturally fractured reservoirs. *In* Proceeedings of the 44th U.S. Rock Mechanics Symposium and 5th U.S.-Canada Rock Mechanics Symposium, Salt Lake City, Utah, June 27–30, 2010.

Dong, C.Y., and de Pater, C.J. 2002. Numerical modeling of crack reorientation and link-up. Advances in Engineering Software, **33**: 577–587. doi:10.1016/S0965-9978(02)00057-1.

Dusseault, M.B., McLennan, J., and Shu, J. 2011. Massive multi-stage hydraulic fracturing for oil 37 and gas recovery from low mobility reservoirs in China. Petroleum Drilling Techniques, **39**(3): 6–16.

Economides, M.J., and Nolte, K.G. 2000. Reservoir stimulation. 3rd ed. John Wiley & Sons.

Geertsma, J., and de Klerk, F. 1969. A rapid method of predicting width and extent of hydraulically induced fractures. Journal of Petroleum Technology, **21**: 1571–1581. doi:10.2118/2458-PA.

Gil, I., Damjanac, B., Nagel, N., and Guo, Q. 2010. Geomechanical evaluation of solids injection. *In* Proceeedings of the 44th U.S. Rock Mechanics Symposium and 5th U.S.-Canada Rock Mechanics Symposium, Salt Lake City, Utah, June 27-30, 2010. ARMA 10-399.

Hamidi, F., and Mortazavi, A. 2012. Three dimensional modeling of hydraulic fracturing process in oil reservoirs. *In* Proceeedings of the 46th U.S. Rock Mechanics/Geomechanics Symposium, Chicago, 24–27 June. ARMA 12-283.

Hazzard, J.F., Young, R.P., and Oates, S.J. 2002. Numerical modeling of seismicity induced by fluid injection in a fractured reservoir. *In* Mining and Tunnel Innovation and Opportunity, Proceedings of the 5th North American Rock Mechanics Symposium, Toronto. University of Toronto Press, pp. 1023–1030.

Hubbert, M.K., and Willis, D.G. 1957. Mechanics of hydraulic fracturing. Journal of Petroleum Technology, **9**(6): 153–66.

Itasca Consulting Group Inc. 2011. UDEC: Universal Distinct Element Code, Version 5.0. ICG, Minneapolis, Minn.

Khristianovitch, S.A. and Zheltov, Y.P. 1955. Formation of vertical fractures by means of highly viscous fluids. In Proceedings of the 4th World Petroleum Congress, Rome. Vol. 2, pp. 579–586.

McLennan, J., Tran, D., Zhao, N., Thakur, S., Deo, M., Gil, I., and Damjanac, B. 2010. Modeling of fluid invasion and hydraulic fracture propagation in naturally fractured rock: a three-dimensional approach. Society of Petroleum Engineers, SPE 127888. doi:10.2118/127888-MS.

Meyer, B.R. 1989. Three-dimensional hydraulic fracturing simulation on personal computers: theory and comparison studies. Society of Petroleum Engineers. SPE 19329. doi:10.2118/19329-MS.

Meyer, B.R., Bazan, L.W., Brown, E.K., and Brinzer, B.C. 2013. Key parameters affecting successful hydraulic fracture design and optimized production in unconventional wells. Society of Petroleum Engineers, SPE 165702. doi:10.2118/165702-MS.

Mohaghegh, S., Balanb, B., Platon, V., and Ameri, S. 1999. Hydraulic fracture design and optimization of gas storage wells. Journal of Petroleum Science and Engineering, **23**(3–4): 161–171. doi:10.1016/S0920-4105(99)00014-5.

Moos, D., and Barton, C.A. 2008. Modelling uncertainty in the permeability of stress-sensitive fractures. *In* Proceeedings of the 42nd U.S. Rock Mechanics Symposium, San Francisco. ARMA 08-312.

Nelson, R.A. 2001. Geological analysis of naturally fractured reservoirs. 2nd ed. Gulf Professional Publishing.

Nordgren, R.P. 1972. Propagation of a vertical hydraulic fracture. SPE Journal, **12**(4): 306–314. doi:10.2118/3009-PA.

Olson, J.E., Bahorich, B., and Holder, J. 2012. Examining hydraulic fracture-natural fracture interaction in hydrostone block experiments. Society of Petroleum Engineers. SPE 15261. doi:10.2118/152618-MS.

Palisch, T., Duenckel, R., Bazan, L., Heidt, H.J. and Turk, G. 2007. Determining realistic fracture conductivity and understanding its impact on well performance – theory and field examples. Society of Petroleum Engineers, SPE 106301. doi:10.2118/106301-MS.

Perkins, T., and Kern, L. 1961. Widths of hydraulic fractures. Journal of Petroleum Technology, **222**: 937–949. doi:10.2118/89-PA.

Reine, C.A., and Dunphy, R.B. 2011. Weighing in on the seismic scale: The use of seismic fault measurements for constructing discrete fracture networks in Horn River Basin. Paper presented at CSPG CSEG CWLS Convention.

Reynolds, M., Shaw, J., and Pollock, B. 2004. Hydraulic fracture design optimi-

zation for deep foothills gas wells. Journal of Canadian Petroleum Technology, **43**(12): 5–11. doi:10.2118/04-12-CS.

Rutledge, J.T., Phillips, W.S., and Mayerhofer, M.J. 2004. Faulting induced by forced fluid injection and fluid flow forced by faulting: an interpretation of hydraulic-fracture microseismicity, Carthage Cotton Valley Gas Field, Texas. Bulletin of the Seismological Society of America, **94**: 1817–1830. doi:10.1785/012003257.

Shaffer, R.J., Thorpe, R.K., Ingraffea, A.R., and Heuze, F.E. 1984. Numerical and physical studies of fluid driven fracture propagation in jointed rock. Society of Petroleum Engineers. SPE 12881-MS. doi:10.2118/12881-MS.

Ventura, J.L. 1985. Slator Ranch fracture optimization study. Journal of Petroleum Technology, **37**(7): 1251–1262. doi:10.2118/12816-PA.

Warpinski, N.R., and Teufel, L.W. 1987. Influence of geologic discontinuities on hydraulic fracture propagation. Journal of Petroleum Technology, **39**(2): 209–220. doi:10.2118/13224-PA.

Warren, W.E., and Smith, C.W. 1985. In situ stress estimates from hydraulic fracturing and direct observation of crack orientation. Journal of Geophysical Research, **90**: 6829–6839. doi:10.1029/JB090iB08p06829.

Wessels, S.A., De La Pena, A., Kratz, M., Williams-Stroud, S., and Jbeili, T. 2011. Identifying faults and fractures in unconventional reservoirs through microseismic monitoring. First Break, **29**: 99–104.

Williams-Stroud, S.C., Barker, W.B. and Smith, K.L. 2012. Induced hydraulic fractures or reactivated natural fractures? Modeling the response of natural fracture networks to stimulation treatments. *In* Proceeedings of the 46th U.S. Rock Mechanics/Geomechanics Symposium, Chicago. ARMA. pp. 12–667.

Yoon, J., Zang, A., and Stephansson, O. 2013. Hydro-mechanical coupled discrete element modeling of geothermal reservoir stimulation and induced seismicity. *In* Clean energy systems in the subsurface: production, storage and conversion. *Edited by* M.Z. Hou, H. Xie, and P. Were. Springer Berlin Heidelberg. pp. 221–231.

Zang, A., Yoon, J.S., Stephansson, O., and Heidbach, O. 2013. Fatigue hydraulic fracturing by cyclic reservoir treatment enhances permeability and reduces induced seismicity. Geophysical Journal International, **195**: 1282–1287. doi:10.1093/gji/ggt301.

Zangeneh, N. 2013. Numerical simulation of hydraulic fracture, stress shadow effects and induced seismicity in jointed rock. Ph.D. thesis, The University of British Columbia.

Zangeneh, N., Eberhardt, E., and Bustin, R.M. 2012. Investigation of the influence of stress shadows on multiple hydraulic fractures from adjacent horizontal wells using the distinct element method. *In* Proceedings, 21st Canadian Rock Mechanics Symposium, RockEng 2012 – Rock Engineering for Natural Resources, Edmonton, 5–9 May. *Edited by* Hawkes et al. Canadian Institute of Mining. pp. 445–454.

Zangeneh, N., Eberhardt, E., Bustin, R.M., and Bustin, A. 2013. A numerical investigation of fault slip triggered by hydraulic fracturing. *In* Effective and sustainable hydraulic fracturing. *Edited by* Bunger et al. InTech Publishers. pp. 477–488.

Zangerl, C., Evans, K.F., Eberhardt, E., and Loew, S. 2008. Normal stiffness of fractures in granitic rock: a compilation of laboratory and in-situ experiments. International Journal of Rock Mechanics and Mining Sciences, **45** (8): 1500–1517.

Zhang, X., Du, C., Deimbacher, F., Crick, M., and Harikesavanallur, A. 2009. Sensitivity studies of horizontal wells with hydraulic fractures in shale gas reservoirs. *In* Proceeedings of the International Petroleum Technology Conference, Dohar, Qatar. IPTC 13338. doi:10.2523/13338-MS.

Zhao, X., and Young, R.P. 2011. Numerical modeling of seismicity induced by fluid injection in naturally fractured reservoirs. Geophysics, **76**: WC167–WC180. doi:10.1190/geo2011-0025.1.

Zoback, M.D. 2007. Reservoir geomechanics. Cambridge University Press.